EU MISSIONS
RESTORE OUR OCEAN AND WATERS

# Scalable full-cycle marine litter remediation in the Mediterranean: Robotic and participatory solutions

SeaClear 2.0

https://www.seaclear2.eu

**D4.2**
**Report on Pose Estimation**
**WP4 — Perception Overhaul**

**Grant Agreement no. 101093822**

Lead beneficiary: TUM

Date: 27/02/2025
Type: R
Dissemination level: PU

## Document information

| | |
|---|---|
| **Grant agreement no.** | 101093822 |
| **Acronym:** | SeaClear2.0 |
| **Full title:** | Scalable full-cycle marine litter remediation in the Mediterranean: Robotic and participatory solutions |
| **Start date of the project** | 01/01/2023 |
| **Duration of the project** | 48 months |
| | |
| **Deliverable** | D4.2: Report on Pose Estimation |
| **Work package** | WP4: Perception Overhaul |
| **Deliverable leader** | TUM |
| **Delivery date** | Contractual: 28/02/2025 Actual: 27/02/2025 |
| **Status** | Draft ☐ Final ✓ |
| **Type**[1] | R ✓ DEM ☐ OTHER ☐ DMP ☐ |
| **Dissemination level**[2] | PU ✓ C-UE/EU-C ☐ SEN ☐ |
| **Author(s)** | Stefan Sosnowski (Technical University of Munich)<br>Cosmin Delea (Fraunhofer)<br>Lucian Busoniu (Universitatea Tehnica Cluj-Napoca) |
| **Responsible author** | Stefan Sosnowski, email: sosnowski@tum.de<br>Technical University of Munich |
| **Deliverable description** | Report on Pose Estimation. (<=T4.2) |

[1] R = Document, report, DEM = demonstrator, OTHER: Software, technical diagram, etc. DMP = Data Management Plan
[2] PU = Public, C-UE/EU-C = EU Confidential under Decision 2015/444, SEN = Sensitive


Co-funded by the European Union

SeaClear2.0 is co-funded by the European Union under the Horizon Europe Programme (Grant Agreement 101093822). Views and opinions expressed herein are those of the author(s) and do not necessarily reflect those of the European Union or European Climate, Infrastructure and Environment Executive Agency (CINEA). Neither the European Union nor the granting authority can be held responsible for them

## Document history

| Name | Date | Version | Description |
|---|---|---|---|
| Stefan Sosnowski | 16/01/2025 | V0.1 | initial draft setup |
| Cosmin Delea | 31/01/2025 | V0.2 | adds USV pose estimation sections |
| Lucian Busoniu | 07/02/2025 | V0.3 | adds ROV pose estimation sections |
| Stefan Sosnowski | 14/02/2025 | V0.4 | Version for internal review |
| Stefan Sosnowski | 27/02/2025 | V1.0 | Final version |


Co-funded by the European Union

SeaClear2.0 is co-funded by the European Union under the Horizon Europe Programme (Grant Agreement 101093822). Views and opinions expressed herein are those of the author(s) and do not necessarily reflect those of the European Union or European Climate, Infrastructure and Environment Executive Agency (CINEA). Neither the European Union nor the granting authority can be held responsible for them

## Disclaimer of warranties

This document has been prepared by SeaClear2.0 project partners as an account of work carried out within the framework of Grant Agreement no. 101093822. Neither the Project Coordinator, nor any signatory party of the SeaClear2.0 Project Consortium Agreement, nor any person acting on behalf of any of them:

- makes any warranty or representation whatsoever, express or implied, with respect to the use of any information, apparatus, method, process, or similar item disclosed in this document, including merchantability and fitness for a particular purpose, that such use does not infringe on or interfere with privately owned rights, including any party's intellectual property; or
- makes any warranty or representation whatsoever, express or implied, that this document is suitable to any particular user's circumstance; or
- assumes responsibility for any damages or other liability whatsoever (including any consequential damages, even if the Project Coordinator or any representative of a signatory party of the Project Consortium Agreement, has been advised of the possibility of such damages) resulting from your selection or use of this document or any information, apparatus, method, process, or similar item disclosed in this document.

SeaClear2.0 is co-funded by the European Union under the Horizon Europe Programme (Grant Agreement 101093822). Views and opinions expressed are those of the author(s) and do not necessarily reflect those of the European Union or European Climate, Infrastructure and Environment Executive Agency (CINEA). Neither the European Union nor the granting authority can be held responsible for them.

## Table of Contents


**Definitions** . . . . . 6

**Abbreviations** . . . . . 6

**Executive Summary** . . . . . 9

**1 Introduction - SeaClear 2.0 at a Glance** . . . . . 10

**2 Theoretical Background on Extended Kalman Filtering** . . . . . 11

**3 System Models and Sensors** . . . . . 13
- 3.1 Surface Vehicles . . . . . 13
  - 3.1.1 Hydrodynamic models . . . . . 13
  - 3.1.2 Kinematics . . . . . 15
  - 3.1.3 Dynamics . . . . . 15
  - 3.1.4 SeaDragon USV control . . . . . 16
- 3.2 Underwater Vehicles . . . . . 16
  - 3.2.1 Mathematical models for filtering . . . . . 16
  - 3.2.2 Shore-cam-based positioning of the underwater vehicle . . . . . 18
  - 3.2.3 Multiple-IMU position estimation . . . . . 19
- 3.3 Smart Grapple System . . . . . 20

**4 Pose Estimation Results** . . . . . 23
- 4.1 USV Pose Estimation . . . . . 23
  - 4.1.1 Experimental setup and preliminaries . . . . . 23
  - 4.1.2 Results . . . . . 26
- 4.2 ROV Pose Estimation . . . . . 28
  - 4.2.1 Main results . . . . . 28
  - 4.2.2 Results using acceleration measurements from the IMU . . . . . 30
- 4.3 Simulated Pose Estimation Results for the Smart Grapple . . . . . 32

**5 Conclusions** . . . . . 35

**References** . . . . . 36

**A SeaDragon Unmanned Surface Vehicle (USV) parameters** . . . . . 37

## Definitions

- **Beneficiary:** A legal entity that is signatory of the EC Grant Agreement no. 101093822.
- **Consortium:** The SeaClear2.0 Consortium, comprising the below-mentioned list of beneficiaries.
- **Consortium Agreement:** Agreement concluded amongst SeaClear2.0 Beneficiaries for the implementation of the Grant Agreement.
- **Grant Agreement:** The agreement signed between the beneficiaries and the EC for the undertaking of the SeaClear 2.0 project (Grant Agreement no. 101093822).

Beneficiaries of the SeaClear2.0 Consortium are referred to herein according to the following abbreviations:

- **TU Delft:** TECHNISCHE UNIVERSITEIT DELFT
- **DUNEA:** REGIONALNA AGENCIJA DUNEA
- **Fraunhofer:** FRAUNHOFER GESELLSCHAFT ZUR FORDERUNG DER ANGEWANDTEN FORSCHUNG EV
- **HPA:** HAMBURG PORT AUTHORITY
- **ISOTECH**: ISOTECH LTD
- **MDanchor**: M. DANCHOR LTD
- **Subsea Tech:** SUBSEA TECH SAS
- **TECNOSUB**: TÉCNICAS Y OBRAS SUBACUÁTICAS, SLU
- **TUM**: TECHNISCHE UNIVERSITAET MUENCHEN
- **UNIDU:** SVEUCILISTE U DUBROVNIKU
- **UTC**: UNIVERSITATEA TEHNICA CLUJ-NAPOCA
- **VEO**: VEOLIA PROPRETE
- **VLPF**: VENICE LAGOON PLASTIC FREE


Co-funded by the European Union

SeaClear2.0 is co-funded by the European Union under the Horizon Europe Programme (Grant Agreement 101093822). Views and opinions expressed herein are those of the author(s) and do not necessarily reflect those of the European Union or European Climate, Infrastructure and Environment Executive Agency (CINEA). Neither the European Union nor the granting authority can be held responsible for them

## Abbreviations

**DOF** Degrees of Freedom. 13–15

**DOP** Dilution of Precision. 25

**DVL** Doppler Velocity Logger. 29, 31, 32, 34

**EKF** Extended Kalman Filter. 11, 24, 29, 30, 32–34

**EOM** Equations of Motion. 13

**GBAS** ground-based augmentation system. 24

**GDOP** Geometric Dilution of Precision. 25

**GNSS** Global Navigation Satellite System. 24–26

**GPS** Global Positioning System. 32, 34

**HDOP** Horizontal Dilution of Precision. 25

**IMU** Inertial Measurement Unit. 16–20, 31–34

**INS** Inertial Navigation Systems. 24, 26

**KPI** Key Performance Indicator. 30

**LiDAR** Light Detection and Ranging. 26

**MARUS** MArine Robotic Unity Simulator. 32–34

**NED** North-East-Down. 24

**PDOP** Position Dilution of Precision. 25

**RMSE** Root Mean Square Error. 33

**ROS** Robot Operating System. 32, 33

**ROV** Remotely Operated Vehicle. 9, 10, 16, 18, 19, 28–31

**RTK** Real-Time Kinematics. 24

**SBL** Short Baseline. 17, 20, 28–33

**SNAME** Society of Naval Architects and Marine Engineers. 13

**UAV** Unmanned Aerial Vehicle. 17, 18, 20, 28, 30

Co-funded by the European Union

SeaClear2.0 is co-funded by the European Union under the Horizon Europe Programme (Grant Agreement 101093822). Views and opinions expressed herein are those of the author(s) and do not necessarily reflect those of the European Union or European Climate, Infrastructure and Environment Executive Agency (CINEA). Neither the European Union nor the granting authority can be held responsible for them

**USBL** Ultra-Short Baseline. 17, 20, 28–30, 33

**USG** underwater smart grapple system. 9, 20–22

**USV** Unmanned Surface Vehicle. 5, 9, 10, 13–16, 20–24, 26, 27, 33, 37

**UUV** Unmanned Underwater Vehicle. 20–22

**VDOP** Vertical Dilution of Precision. 25



Co-funded by the European Union

SeaClear2.0 is co-funded by the European Union under the Horizon Europe Programme (Grant Agreement 101093822). Views and opinions expressed herein are those of the author(s) and do not necessarily reflect those of the European Union or European Climate, Infrastructure and Environment Executive Agency (CINEA). Neither the European Union nor the granting authority can be held responsible for them

## Executive Summary


This document is part of the SeaClear 2.0 project, which aims to develop an autonomous robotic systems for marine litter collection. The report focuses on the advancements in pose estimation techniques for various robotic components used in the project, including USVs, Remotely Operated Vehicles (ROVs), and the underwater smart grapple system (USG).

This document will detail the methodologies, system models, sensor integrations, and experimental results related to pose estimation.

**Key Points**

1. **Theoretical Background**

   The document provides an overview of the theoretical principles underlying pose estimation for generic mobile systems, which form the basis for specific filter structures in the next section, including kinematic and dynamic models for surface and underwater vehicles.

2. **System Models and Sensors**

   Detailed descriptions of the models and sensors used for pose estimation in surface vehicles (USVs), underwater vehicles (ROVs), and the USG, including hydrodynamic models, kinematics, dynamics, and sensor fusion techniques.

3. **Experimental Results**

   The report presents the results of various experiments conducted to validate the pose estimation techniques.

   - This includes:
     - MiniTortuga ROV experiments to compare different acoustic positioning sensors and their performance, as well as to validate the pose estimation pipeline.
     - USV pose estimation trials to evaluate the performance of the pose estimation system in real-world scenarios.
     - A simulation-based evaluation of the pose estimation for the smart grapple system.

4. **Conclusion**

   The experimental results demonstrate the effectiveness of the proposed techniques and provide a foundation for further improvements and integration into the overall system.



Co-funded by the European Union

SeaClear2.0 is co-funded by the European Union under the Horizon Europe Programme (Grant Agreement 101093822). Views and opinions expressed herein are those of the author(s) and do not necessarily reflect those of the European Union or European Climate, Infrastructure and Environment Executive Agency (CINEA). Neither the European Union nor the granting authority can be held responsible for them

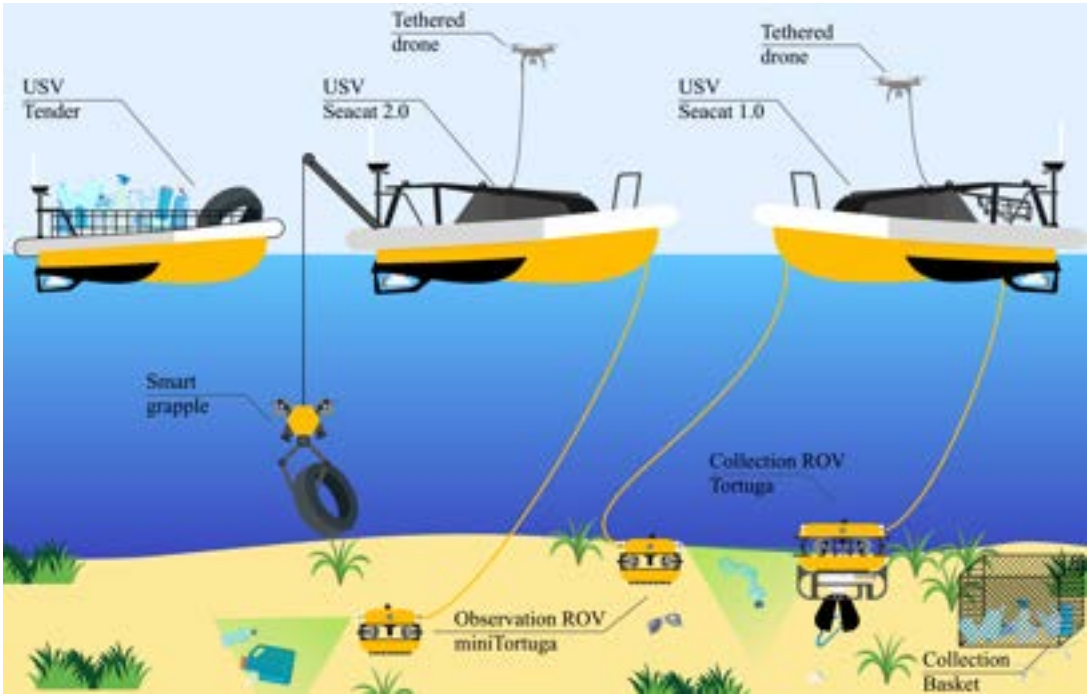



Figure 1: Concept of SeaClear 2.0 robotic system (left/middle) and SeaClear 1.0 (right)

# 1 Introduction - SeaClear 2.0 at a Glance

SeaClear 2.0 is the next step to the H2020-funded SeaClear (https://seaclear-project.eu), where several of the SeaClear2.0 partners have been developing the first autonomous robotic system for seafloor litter collection. An USV called SeaCAT acts as a hub for an unmanned aerial vehicle (UAV) that searches for litter from the air and contributes to situational awareness, an observation ROV called Mini-Tortuga that searches for litter underwater, and a collection ROV called Tortuga that collects the litter with a custom gripper plus-suction device and deposits it in a basket lowered from the USV. The very nature of SeaClear (labelled 1.0 in the document) as the first project to design such a solution means it must focus almost exclusively on technological developments in robotics hardware and algorithms, with a single system.

Moreover, the system is limited to only seafloor litter of up to tens of centimeters in size and at depths of up to tens of meters; it cannot collect surface litter or larger objects like fishing equipment, bikes, e-scooters, tires, shipping equipment, etc, which SeaClear 1.0 identified as a significant subset of the litter in industrial port or mariculture settings. The aim of SeaClear 2.0 is to upscale and upgrade the system initially made for SeaClear 1.0. This means collecting bigger and heavier litter with a modified SeaCAT2 and a smart grapple, storing and shipping it to shore with a dedicated USV Tender, as well as collecting surface litter with a USV and a team of highly manoeuvrable surface robots. In the end, SeaClear 1.0 and SeaClear 2.0 will be working together, exploiting their shared and complementary litter detection and collection capabilities.


Co-funded by the European Union

SeaClear2.0 is co-funded by the European Union under the Horizon Europe Programme (Grant Agreement 101093822). Views and opinions expressed herein are those of the author(s) and do not necessarily reflect those of the European Union or European Climate, Infrastructure and Environment Executive Agency (CINEA). Neither the European Union nor the granting authority can be held responsible for them

## 2 Theoretical Background on Extended Kalman Filtering

Pose estimation for the heterogeneous multi-robot system in SeaClear2.0 is conducted under the same assumptions for all components: that observations and measurements of states of the systems are imperfect, i.e., subject to noise, and that motion models exhibit nonlinear characteristics. In order to improve the estimation of the pose we use the de-facto standard Kalman filter for guidance, navigation and control of the robotic systems. Specifically, we use its variant called the Extended Kalman Filter (EKF) due to the nonlinearity in the state transition models. The remainder of this section introduces the common theoretical framework of the EKF for all components in SeaClear2.0, with the individual system models later introduced in Section 3.

The Extended Kalman Filter (EKF) is a typical approach for state estimation of nonlinear systems. By linearizing the dynamics model at each time step, the system states are first predicted, and then corrected with the measurement, using equations similar to those of the standard Kalman Filter. The nonlinear system is defined as a discrete-time form:

$$\begin{aligned} &\boldsymbol{x}_k = \boldsymbol{f}(\boldsymbol{x}_{k-1}, \boldsymbol{u}_{k-1}) + \boldsymbol{v}_{k-1}, \boldsymbol{v}_{k-1} \sim \mathcal{N}(0, \boldsymbol{Q}_k) \\ &\boldsymbol{y}_k = \boldsymbol{h}(\boldsymbol{x}_k) + \boldsymbol{w}_k, \boldsymbol{w}_k \sim \mathcal{N}(0, \boldsymbol{R}_k) \quad \boldsymbol{x}_k \in \mathbb{R}^n, \boldsymbol{u}_k \in \mathbb{R}^m, \boldsymbol{y}_k \in \mathbb{R}^p, m, n, p \in \mathbb{N} \end{aligned} \tag{1}$$

where $\boldsymbol{x}_k$ and $\boldsymbol{u}_k$ are system states and control inputs at the discrete time step $k$, respectively, $\boldsymbol{y}_k$ represents the vector of measurement, $\boldsymbol{f}(\cdot,\cdot,\cdot) \in \mathbb{R}^n \times \mathbb{R}^m \to \mathbb{R}^n$ are non-linear functions that characterize the system dynamics, and $\boldsymbol{h} \in \mathbb{R}^n \to \mathbb{R}^p$ is the relationship between system states and the measurement. To formulate the uncertainty of the system dynamics as well as measurement noise, the Gaussian noise $\boldsymbol{v}_k$ with its covariance matrices $\boldsymbol{Q}_k \in \mathbb{R}^{n\times n}$ and the Gaussian noise $\boldsymbol{w}_k$ with its covariance matrices $\boldsymbol{R}_k \in \mathbb{R}^{p\times p}$ is introduced in (1).

The estimation is constructed by the following two stages:

1. Prediction: predict the state based on prior knowledge
2. Correction: provide the final estimation by modifying the prediction based on measurements.

In the prediction stage, the system dynamics (1) are linearized by leveraging the Taylor expansion, and the states at the current step $k$ are predicted by the linearized system $\boldsymbol{f}_l(\cdot,\cdot)$ applied to the estimated states $\boldsymbol{x}_{k-1} \sim \mathcal{N}(\boldsymbol{\mu}_{k-1}, \boldsymbol{P}_{k-1})$ at the last step

$$\begin{aligned} &\hat{\boldsymbol{x}}_k \approx \boldsymbol{f}_l(\boldsymbol{x}_{k-1}, \boldsymbol{u}_{k-1}) \sim \mathcal{N}(\hat{\boldsymbol{\mu}}_k, \hat{\boldsymbol{P}}_k) \\ &\boldsymbol{f}_l(\boldsymbol{x}_{k-1}, \boldsymbol{u}_{k-1}) = \boldsymbol{f}(\boldsymbol{\mu}_{k-1}, \boldsymbol{u}_{k-1}) + \boldsymbol{A}_{k-1}(\boldsymbol{x}_{k-1} - \boldsymbol{\mu}_{k-1}) + \boldsymbol{v}_{k-1} \end{aligned} \tag{2}$$

where $\boldsymbol{A}_k \in \mathbb{R}^{n\times n}$ is the Jacobian matrix of nonlinear dynamics $\boldsymbol{f}(\cdot,\cdot,\cdot)$. It is important to note that the states at each step are formulated as random variables governed by a Gaussian distribution, where the mean is utilized as the estimated state. The mean $\hat{\boldsymbol{\mu}}_k \in \mathbb{R}^n$ and the variance $\hat{\boldsymbol{P}}_k \in \mathbb{R}^{n\times n}$ of the predicted state $\hat{\boldsymbol{x}}_k$ are written as follows

$$\hat{\boldsymbol{\mu}}_k = \mathbb{E}[\hat{\boldsymbol{x}}_k] = \boldsymbol{f}(\boldsymbol{\mu}_{k-1}, \boldsymbol{u}_{k-1}) + \boldsymbol{A}_{k-1}\mathbb{E}[\boldsymbol{x}_{k-1} - \boldsymbol{\mu}_{k-1}] + \mathbb{E}[\boldsymbol{v}_{k-1}] = \boldsymbol{f}(\boldsymbol{\mu}_{k-1}, \boldsymbol{u}_{k-1}) \tag{3}$$

$$\hat{\boldsymbol{P}}_k = \mathrm{Var}(\hat{\boldsymbol{x}}_k) = \mathrm{Var}(\boldsymbol{A}_{k-1}(\boldsymbol{x}_{k-1} - \boldsymbol{\mu}_{k-1}) + \boldsymbol{v}_{k-1}) = \boldsymbol{A}_{k-1}\boldsymbol{P}_{k-1}\boldsymbol{A}_{k-1}^T + \boldsymbol{Q}_{k-1} \tag{4}$$

Co-funded by the European Union

SeaClear2.0 is co-funded by the European Union under the Horizon Europe Programme (Grant Agreement 101093822). Views and opinions expressed herein are those of the author(s) and do not necessarily reflect those of the European Union or European Climate, Infrastructure and Environment Executive Agency (CINEA). Neither the European Union nor the granting authority can be held responsible for them

Following the same idea of linearizing the system by a Taylor expansion, the predicted measurement can be represented below

$$\hat{\boldsymbol{y}}_k = \boldsymbol{h}(\hat{\boldsymbol{x}}_k) \approx \boldsymbol{h}(\hat{\boldsymbol{\mu}}_k) + \boldsymbol{H}_k(\hat{\boldsymbol{x}} - \hat{\boldsymbol{\mu}}_k) \sim \mathcal{N}(\boldsymbol{h}(\hat{\boldsymbol{\mu}}_k), \boldsymbol{H}_k\hat{\boldsymbol{P}}_k\boldsymbol{H}_k^T) \tag{5}$$

where $\boldsymbol{H}_k \in \mathbb{R}^{p\times n}$ is the Jacobian matrix of $\boldsymbol{h}(\cdot)$. After obtaining the predicted measurement (5), the real measurement $\tilde{\boldsymbol{y}}_k$ is obtained from the sensor and written as follows

$$\tilde{\boldsymbol{y}}_k \sim \mathcal{N}(\boldsymbol{z}_k, \boldsymbol{R}_k) \tag{6}$$

where $\boldsymbol{R}_k$ is the variance of the measurement noise.

The predicted measurement (5) is viewed as the prior distribution $p(A) = \hat{\boldsymbol{y}}_k$, and the real measurement (6) is viewed as likelihood $p(B|A) = \tilde{\boldsymbol{y}}_k$ since the measurement is obtained after the state observation. With the Bayesian Theorem, the posterior distribution $\boldsymbol{y}_k$ is obtained by $\boldsymbol{y}_k = p(A|B) \propto p(B|A)p(A) = \tilde{\boldsymbol{y}}_k\hat{\boldsymbol{y}}_k$. As both $p(A)$ and $p(B|A)$ are Gaussian distributions, their product is still a Gaussian distribution

$$\mathcal{N}(\boldsymbol{\mu}_1, \boldsymbol{\Sigma}_1) \times \mathcal{N}(\boldsymbol{\mu}_2, \boldsymbol{\Sigma}_2) = \mathcal{N}(\frac{\boldsymbol{\mu}_1\boldsymbol{\Sigma}_2 + \boldsymbol{\mu}_2\boldsymbol{\Sigma}_1}{\boldsymbol{\Sigma}_1 + \boldsymbol{\Sigma}_2}, \frac{\boldsymbol{\Sigma}_1\boldsymbol{\Sigma}_2}{\boldsymbol{\Sigma}_1 + \boldsymbol{\Sigma}_2}). \tag{7}$$

In the corrected stage, the mean and variance of $\boldsymbol{y}_k$ are updated by multiplying $\tilde{\boldsymbol{y}}_k$ as well as $\hat{\boldsymbol{y}}_k$ and are derived as

$$\boldsymbol{\mu}_{\boldsymbol{y},k} = \boldsymbol{h}(\hat{\boldsymbol{\mu}}_k) + \boldsymbol{H}_k(\boldsymbol{\mu}_k - \hat{\boldsymbol{\mu}}_k) = \frac{\boldsymbol{R}_k\boldsymbol{h}(\hat{\boldsymbol{\mu}}_k) + \boldsymbol{H}_k\hat{\boldsymbol{P}}_k\boldsymbol{H}_k^T\boldsymbol{z}_k}{\boldsymbol{H}_k\hat{\boldsymbol{P}}_k\boldsymbol{H}_k^T + \boldsymbol{R}_k} \tag{8}$$

$$\boldsymbol{P}_{\boldsymbol{y},k} = \boldsymbol{H}_k\boldsymbol{P}_k\boldsymbol{H}_k^T = \frac{\boldsymbol{H}_k\hat{\boldsymbol{P}}_k\boldsymbol{H}_k^T\boldsymbol{R}_k}{\boldsymbol{H}_k\hat{\boldsymbol{P}}_k\boldsymbol{H}_k^T + \boldsymbol{R}_k} \tag{9}$$

. The updated estimated state $\boldsymbol{x}_k \sim \mathcal{N}(\boldsymbol{\mu}_k, \boldsymbol{P}_k)$ is written as

$$\boldsymbol{\mu}_k = \hat{\boldsymbol{\mu}}_k + \boldsymbol{K}_k(\boldsymbol{z}_k - \boldsymbol{h}(\hat{\boldsymbol{\mu}}_k)) \tag{10}$$

$$\boldsymbol{P}_k = (\boldsymbol{I} - \boldsymbol{K}_k\boldsymbol{H}_k)\hat{\boldsymbol{P}}_k \tag{11}$$

$$\boldsymbol{K}_k = \frac{\hat{\boldsymbol{P}}_k\boldsymbol{H}_k^T}{\boldsymbol{H}_k\hat{\boldsymbol{P}}_k\boldsymbol{H}_k^T + \boldsymbol{R}_k} \tag{12}$$

The Gaussian distribution of the final estimated state can be updated based on the prediction result. Note that the state transitions and measurement functions can be derived from motion and system models of the respective observed dynamical systems. We will introduce these system models in the next section.

Co-funded by the European Union

SeaClear2.0 is co-funded by the European Union under the Horizon Europe Programme (Grant Agreement 101093822). Views and opinions expressed herein are those of the author(s) and do not necessarily reflect those of the European Union or European Climate, Infrastructure and Environment Executive Agency (CINEA). Neither the European Union nor the granting authority can be held responsible for them

# 3 System Models and Sensors

This section introduces the individual motion models and the suite of sensors for pose estimation filters.

## 3.1 Surface Vehicles

In the SeaClear2.0 system, the SeaDragon USV, the SeaCAT USV and the surface collection system behave according to the following motion models. We will exemplarily look into the SeaDragon model, with direct transferability to the other surface systems.

### 3.1.1 Hydrodynamic models

For marine vessels moving in six Degrees of Freedom (DOF), six independent coordinates are required to determine their position and orientation. The first three coordinates and their time derivatives correspond to the position and translational motion along the x, y, and z axes, while the last three coordinates and their time derivatives describe orientation and rotational motion [1]. According to the Society of Naval Architects and Marine Engineers (SNAME) [2], the six different motion components are conventionally defined as surge, sway, heave, roll, pitch, and yaw (see Figure 2 and Table 1).

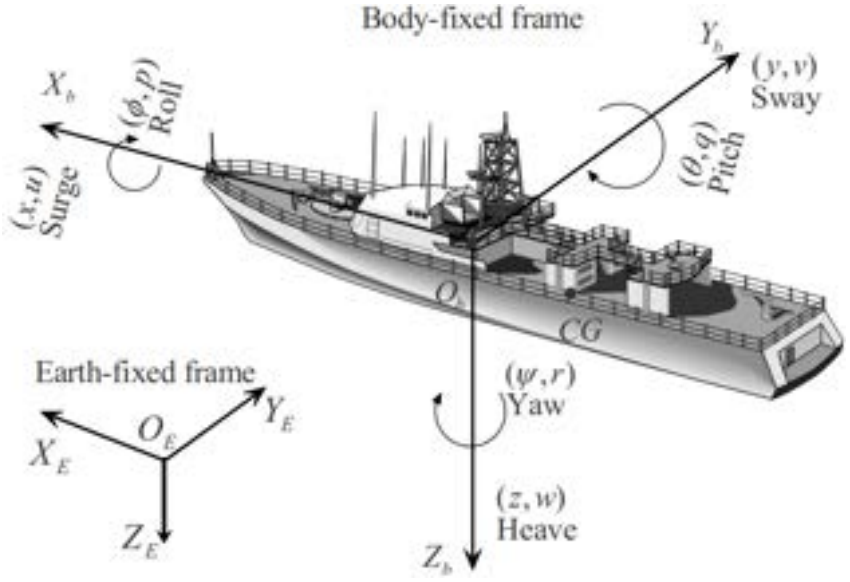



Figure 2: Motion variables for an ocean vessel [1]

The complete Equations of Motion (EOM) for a 6 DOF system include multiple nonlinearities, such as hydrostatic effects, cross-flow drag, and nonlinear damping, but this representation is highly complex and suboptimal for controlling underactuated ships. Even with azimuth thrusters, there are only 4 control inputs (speed and angle of each thruster), while the heave motion (translation on the normal axis to the vessel) is not controllable. Typically, the motion of a surface vessel moving in a horizontal plane is often described by the motion components in surge, sway, and yaw. The simplified three DOF USV model can be obtained under the following assumptions [3]:

Co-funded by the European Union

SeaClear2.0 is co-funded by the European Union under the Horizon Europe Programme (Grant Agreement 101093822). Views and opinions expressed herein are those of the author(s) and do not necessarily reflect those of the European Union or European Climate, Infrastructure and Environment Executive Agency (CINEA). Neither the European Union nor the granting authority can be held responsible for them

Table 1: The SNAME notations for marine vessels, source [2]

| Degree of freedom | Force and moment | Linear and angular velocity | Position and Euler angles |
|---|---|---|---|
| 1 surge | X | u | x |
| 2 sway | Y | v | y |
| 3 heave | Z | w | z |
| 4 roll | K | p | $\phi$ |
| 5 pitch | M | q | $\theta$ |
| 6 yaw | N | r | $\psi$ |

- The vessel has three planes of symmetry.
- The mass distribution is homogeneous.
- The pitch and roll motions are neglected.

Therefore, a more appropriate linear 3 DOF horizontal plane model that only includes surge, sway, and yaw dynamics is used for the vessel model in the following sections. Nevertheless, all 6 DOF need be monitored in some situations, due to safety considerations. In the scenario envisioned in SeaClear2.0, the docking and transboarding procedure of the SeaDragon USV to the SeaCat2 USV encompass the risks of collisions and capsizing between the two, hence the heave, roll and pitch DOF will be monitored and kept within certain limits through an operator remotely overtaking control, if this will be required.

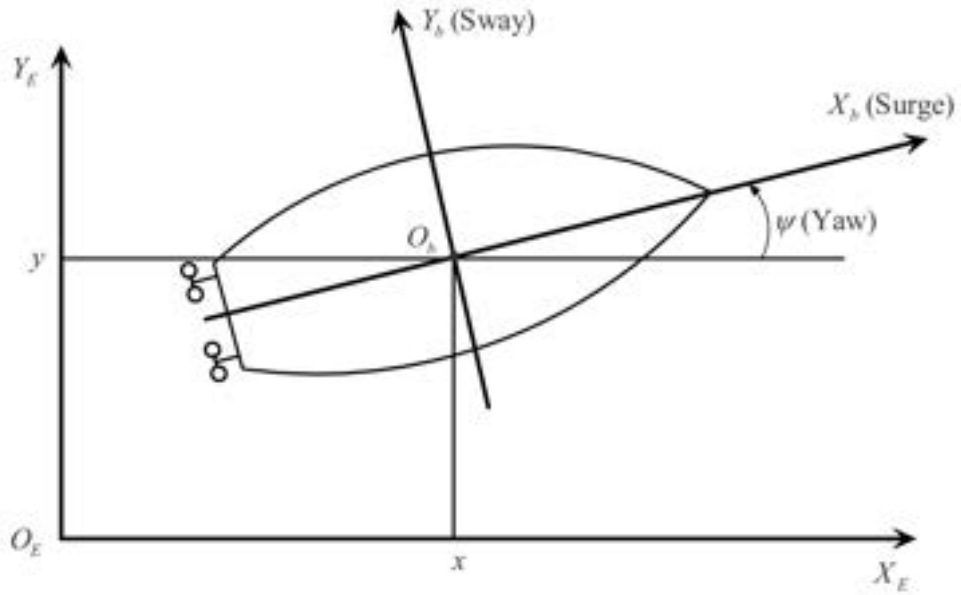



Figure 3: Motion variables for an ocean vessel moving in a horizontal plane [1]


Co-funded by the European Union

SeaClear2.0 is co-funded by the European Union under the Horizon Europe Programme (Grant Agreement 101093822). Views and opinions expressed herein are those of the author(s) and do not necessarily reflect those of the European Union or European Climate, Infrastructure and Environment Executive Agency (CINEA). Neither the European Union nor the granting authority can be held responsible for them

### 3.1.2 Kinematics

The kinematics of the USV in the local horizontal plane are described by the velocity vector $\mathbf{v} = [u, v, r]^\top$ representing surge, sway, and yaw velocities, respectively. The position and orientation vector $\boldsymbol{\eta} = [x, y, \psi]^\top$ includes the coordinates and heading angle of the vessel. The kinematic equations governing the vessel's motion are expressed as follows [1, 4]:

$$\dot{\eta} = \mathbf{R}(\psi)\mathbf{v} \tag{13}$$

where $\mathbf{R}(\psi)$ is the rotation matrix transforming body reference frame velocities to the inertial reference frame, satisfying the orthogonality condition:

$$\mathbf{R}(\psi)^T\mathbf{R}(\psi) = I \quad \forall\psi \tag{14}$$

This matrix accounts for the heading angle $\psi$, facilitating the conversion between coordinate frames.

The 3 DOF kinematic equations can be described as follows:

$$\dot{\eta} = \begin{bmatrix} \cos\psi & -\sin\psi & 0 \\ \sin\psi & \cos\psi & 0 \\ 0 & 0 & 1 \end{bmatrix} \begin{bmatrix} u \\ v \\ r \end{bmatrix} = \mathbf{R}(\psi)\mathbf{v}. \tag{15}$$

### 3.1.3 Dynamics

Most ships have port/starboard symmetry but fore/aft non-symmetry. This non-symmetry leads to the nonzero off-diagonal terms in the inertia and damping matrices. However, these terms are small compared to the main diagonal terms [5].

Therefore, the dynamics equations of motion are given by [1]:

$$\mathbf{M}\dot{\mathbf{v}} = -\mathbf{C}(\mathbf{v})\mathbf{v} - \mathbf{D}\mathbf{v} + \tau + \mathbf{w}, \tag{16}$$

where the matrices $\mathbf{M}$, $\mathbf{C}(\mathbf{v})$ and $\mathbf{D}$ are given by:

$$\mathbf{M} = \begin{bmatrix} m_{11} & 0 & 0 \\ 0 & m_{22} & 0 \\ 0 & 0 & m_{33} \end{bmatrix}, \quad \mathbf{C}(\mathbf{v}) = \begin{bmatrix} 0 & 0 & -m_{22}v \\ 0 & 0 & m_{11}u \\ m_{22}v & -m_{11}u & 0 \end{bmatrix}, \quad \mathbf{D} = \begin{bmatrix} d_{11} & 0 & 0 \\ 0 & d_{22} & 0 \\ 0 & 0 & d_{33} \end{bmatrix}, \tag{17}$$

where

Co-funded by the European Union

SeaClear2.0 is co-funded by the European Union under the Horizon Europe Programme (Grant Agreement 101093822). Views and opinions expressed herein are those of the author(s) and do not necessarily reflect those of the European Union or European Climate, Infrastructure and Environment Executive Agency (CINEA). Neither the European Union nor the granting authority can be held responsible for them

$$m_{11} = m - X_{\dot{\mathbf{u}}}, \quad m_{22} = m - Y_{\dot{\mathbf{v}}}, \quad m_{33} = I_{\mathbf{z}} - N_{\dot{\mathbf{r}}}, \tag{18}$$

$$d_{11} = -X_{\mathbf{u}}, \quad d_{22} = -Y_{\mathbf{v}}, \quad d_{33} = -N_{\mathbf{r}}. \tag{19}$$

Determination of the full dynamics parameters is an ongoing process in the field experiments with the SeaDragon USV. A selection of estimates is provided in Table 4 in the appendix.

#### 3.1.4 SeaDragon USV control

USVs are classified as nonholonomic when they do not have independent actuators for managing sway and heave motions, resulting in nonintegrable second-order differential constraints on their configuration variables [1]. These nonholonomic constraints restrict the vessels' immediate maneuverability and pose challenges in the design of feedback controllers. Nevertheless, they still allow almost global controllability within their operational domains [1]. The higher manoeuvrability of the vessel is needed in the SeaClear2.0 scenario during docking and unloading procedure. During these procedures, the vessel needs to correct its pose and remain aligned with the SeaCat2 USV while being impacted by environmental disturbances (wind, currents). As a mechanical coupling between the two vessels has been ruled out due to the risks of losing manoeuvrability and damaging one another, only loose mechanical couplings have been allowed. Hence, having the possibility to adjust to possible drifts on the sway direction is highly needed. In addition, for docking on moving targets, which could be a use-case for SeaClear2.0 in the case where the target USVs are unable to do station keeping, the need of a trajectory-based approach is highly needed. As mentioned in [4], trajectory control of an USV is difficult to achieve without an overactuated system. Full actuation is accomplished for the SeaDragon USV by using azimuth thrusters. This involves a twin-propeller mounted at the stern of the vessel, capable of adjusting the water vortex relative to the normal axis of the marine craft.

### 3.2 Underwater Vehicles

We present in turn the models used for the ROV in the system, a way to determine its position from a shore-based camera, and a platform for evaluating the benefits of using multiple Inertial Measurement Unit (IMU)s.

#### 3.2.1 Mathematical models for filtering

For the MiniTortuga ROV, the baseline model that we use is – like in SeaClear – a six degree-of-freedom (6-DOF) constant-acceleration kinematic model. The state vector is:

$$\boldsymbol{x} = [x, y, z, \phi, \theta, \psi, v_x, v_y, v_z, v_\phi, v_\theta, v_\psi, a_x, a_y, a_z]^T \tag{20}$$

Co-funded by the European Union

SeaClear2.0 is co-funded by the European Union under the Horizon Europe Programme (Grant Agreement 101093822). Views and opinions expressed herein are those of the author(s) and do not necessarily reflect those of the European Union or European Climate, Infrastructure and Environment Executive Agency (CINEA). Neither the European Union nor the granting authority can be held responsible for them

where $x, y, z$ are Cartesian coordinates, $\phi, \theta, \psi$ are Euler angles, while $v_*$ and $a_*$ are the velocity and acceleration of variable '$*$', respectively. The discrete-time dynamics, obtained by Euler integration, are:

$$f(\boldsymbol{x}) = \boldsymbol{x} + T_s \begin{bmatrix} v_x \cos\theta\cos\psi + v_y(-\cos\phi\sin\psi + \sin\phi\sin\theta\cos\psi) + v_z(\sin\phi\sin\psi + \cos\phi\sin\theta\cos\psi) \\ v_x \cos\theta\sin\psi + v_y(\cos\phi\cos\psi + \sin\phi\sin\theta\sin\psi) + v_z(-\sin\phi\cos\psi + \cos\phi\sin\theta\sin\psi) \\ -v_x\sin\theta + v_y\sin\phi\cos\theta + v_z\cos\phi\cos\theta \\ v_\phi + v_\theta\sin\phi\tan\theta + v_\psi\cos\phi\tan\theta \\ v_\theta\cos\phi - v_\psi\sin\phi \\ v_\theta\sin\phi/\cos\theta + v_\psi\cos\phi/\cos\theta \\ a_x \\ a_y \\ a_z \\ 0_{6\times 1} \end{bmatrix} \tag{21}$$

where $T_s$ is the sampling period and $0_{6\times 1}$ denotes a column vector of six zeros.

The state variables are estimated based on the observations of the following sensors:

- Angular positions $\varphi, \theta, \psi$: inertial measurement unit (IMU).
- Linear velocities $v_x, v_y, v_z$: Dopper velocity logger (DVL), specifically the A50 model from Water-Linked.
- Vertical position $z$: pressure sensor.
- Positions $x, y$: several sensors, as discussed next.

A critical sensor for pose (and, later on, mapping) accuracy is the one for absolute position. We use several alternatives for this purpose:

1. An acoustic, Short Baseline (SBL) sensor, specifically the WaterLinked 'Underwater GPS'.
2. An Ultra-Short Baseline (USBL) sensor.
3. A position measured by the Unmanned Aerial Vehicle (UAV) camera.
4. A position measured by a camera placed on the shore.

Sensors 1 and 3 were also used in SeaClear (although UAV-based positioning has been improved since). The new shore-camera-based position is detailed in Section 3.2.2. By running experiments that record several of these sensors at the same time and comparing their outputs, we will later be able to rule out those that have poor performance.

Thus, the system output for filtering consists of $[x, y, z, v_x, v_y, v_z, \varphi, \theta, \psi]^\top$. Measurement covariances are reported by the acoustic sensors, and experimentally tuned for the IMU and for camera-based measurements.

Co-funded by the European Union

SeaClear2.0 is co-funded by the European Union under the Horizon Europe Programme (Grant Agreement 101093822). Views and opinions expressed herein are those of the author(s) and do not necessarily reflect those of the European Union or European Climate, Infrastructure and Environment Executive Agency (CINEA). Neither the European Union nor the granting authority can be held responsible for them

Moreover, and differently from SeaClear, we will also test a model that considers accelerations and angular velocities as inputs and also estimates biases for these signals, by including them in the state vector. The states for this model are:

$$\boldsymbol{x} = [q_0, q_1, q_2, q_3, p_N, p_E, p_D, v_N, v_E, v_D, \\ \delta v_\theta, \delta v_\phi, \delta v_\psi, \delta a_x, \delta a_y, \delta a_z, G_N, G_E, G_D, \delta M_x, \delta M_y, \delta M_z]^\top \quad (22)$$

where $q$ represents an earth-referenced orientation quaternion element, $p$ is the position, $a$ represents the acceleration, $G$ is the estimate of the geomagnetic field at a reference location, and $M$ indicates magnetometer readings. Moreover, $NED$ and $xyz$ subscripts respectively identify the earth-referenced frame and the body frame, while each signal $\delta_*$ is the bias for measurement '$*$'. For the dynamics, see [6]. In addition to the measurements from the list given above, for this filter we also include the linear accelerations reported by the IMU.

### 3.2.2 Shore-cam-based positioning of the underwater vehicle

The UAV camera usually has the best vantage point to see the ROV underwater and a wide field of view; thus, it provides a high-quality position source. However, the UAV is costly to ship and setup, and it requires an always-available operator for legal reasons. So that we can still validate the position when the UAV is not available due to these complications, we also developed an ROV positioning system that uses a shore-mounted camera.

The setup consists of a GoPro Hero 9 camera fixed on the shore at approximately 2.5 meters above ground level. An ArUco marker of size 0.3m is placed at ground level ($z = 0$) to establish the reference coordinate frame. The ROV is detected and its pose is estimated relative to this marker. Using Rodrigues transformations [7], the camera's pose is inverted to be expressed relative to the markers coordinate system.

ROV detection is performed using HSV-based color segmentation, focusing on yellow hues to isolate the ROV. The detected centroid of the segmented region is converted into the marker coordinate system by considering the camera calibration matrix, distortion coefficients, and known depth value provided by the depth sensor from the ROV, as explained in [8]. We use the pinhole camera model, which describes the link between a point $\mathtt{P_w}$ in 3D and its projection $\mathtt{x}, \mathtt{y}$, represented in homogeneous coordinates in the image plane:

$$[\mathtt{x}, \mathtt{y}, 1]^\top = \mathtt{K} \cdot \mathtt{T} \cdot \mathtt{P_w} \quad (23)$$

where $\mathtt{K}$ is the camera intrinsic matrix (obtained via calibration); and $\mathtt{T}$ is the transformation matrix (rotation, translation) between the marker and camera frames.

The procedure is illustrated in Figure 4. We begin with the pixel coordinates $\mathtt{x}, \mathtt{y}$ of the region centroid or the center of the detection bounding box, and multiply these coordinates with the inverse of the camera intrinsic matrix $\mathtt{K}$ to obtain a new set of coordinates that provide the direction $\mathtt{d}$ towards the ROV, in the camera reference frame. This line goes through the center point of camera $\mathtt{C} = [0, 0, 0]^\mathtt{T}$ and intersects both the image of the detected ROV as well as the ROV itself. Next, we transform the camera-frame direction $\mathtt{d}$ to a marker-frame direction $\mathtt{d_w}$ by multiplying with the inverse of the rotation matrix between the camera and marker frames $\mathtt{R}$:

$$\mathtt{d_w} = \mathtt{R}^{-1} \cdot \mathtt{d} \quad (24)$$

Co-funded by the European Union

SeaClear2.0 is co-funded by the European Union under the Horizon Europe Programme (Grant Agreement 101093822). Views and opinions expressed herein are those of the author(s) and do not necessarily reflect those of the European Union or European Climate, Infrastructure and Environment Executive Agency (CINEA). Neither the European Union nor the granting authority can be held responsible for them

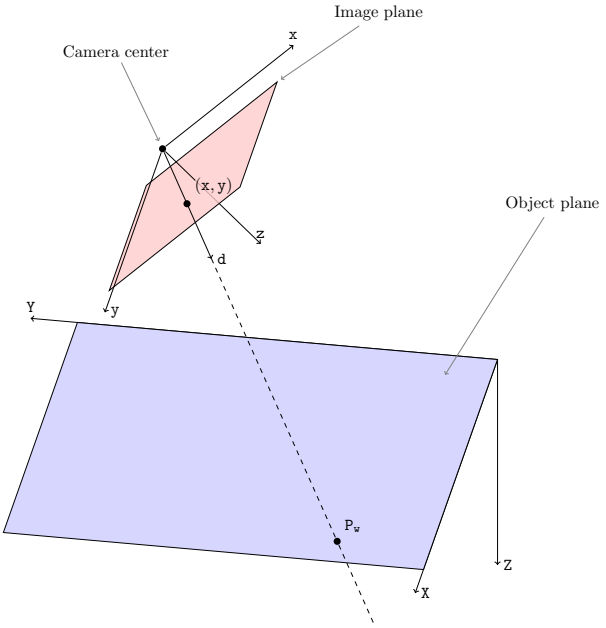



Figure 4: Procedure to find the marker-frame coordinates of the ROV

The marker-frame position of the ROV is given by the intersection of $d_w$ and the horizontal plane of the ROV. The marker coordinate $Z_{w,ROV}$ for this plane represents the depth measured by the pressure sensor, including the additional offset from the water surface to the ground level; note that $Z_w = 0$ at ground level. Further, we require the camera pose, determined with the ArUco marker above. The transformation matrix obtained from the ArUco marker detection is applied to convert the direction into the marker's coordinate frame, ensuring alignment with the predefined reference system.

Finally, the coordinates $X, Y$ of the ROV (belonging to $P_w$), as well as $s$, the distance along direction $d_w$ until the ROV is reached, are determined by solving the system of equations:

$$\begin{cases} P_w = C_w + d_w \cdot s \\ \begin{bmatrix} 0 & 0 & 1 \end{bmatrix} \cdot P_w = Z_{w,ROV} \end{cases} \tag{25}$$

Note that in order to correct for light refraction on the water, Snell's law is applied, modifying the direction vector to account for the change in medium from air to water (this correction is not included in the figure and in the equations).

### 3.2.3 Multiple-IMU position estimation

The MiniTortuga ROV uses a single, relatively low-cost IMU. Using linear accelerations from this IMU, which are biased and noisy, leads to poor estimates affected by drift and random walk. We developed a setup to verify whether adding multiple IMUs - so that we implicitly average their outputs in the filter - helps to address this issue.

Either one or two IMUs (of the type ICM 20948) were connected to a Raspberry PI 4 running Ubuntu Server 18.04. The images in Figure 5 show the RPI with the IMU sensors connected to it. The RPI was


Co-funded by the European Union

SeaClear2.0 is co-funded by the European Union under the Horizon Europe Programme (Grant Agreement 101093822). Views and opinions expressed herein are those of the author(s) and do not necessarily reflect those of the European Union or European Climate, Infrastructure and Environment Executive Agency (CINEA). Neither the European Union nor the granting authority can be held responsible for them

attached to a UR5 robotic arm that was programmed to execute a rectangular trajectory. While the arm executes the trajectory, a ROS bag records the data from the sensors together with the joint states of the arm. Later, the joint states are used to obtain the cartesian coordinates of the end-effector in the robot frame, via the direct geometric model. The resulting position is used as a reference.

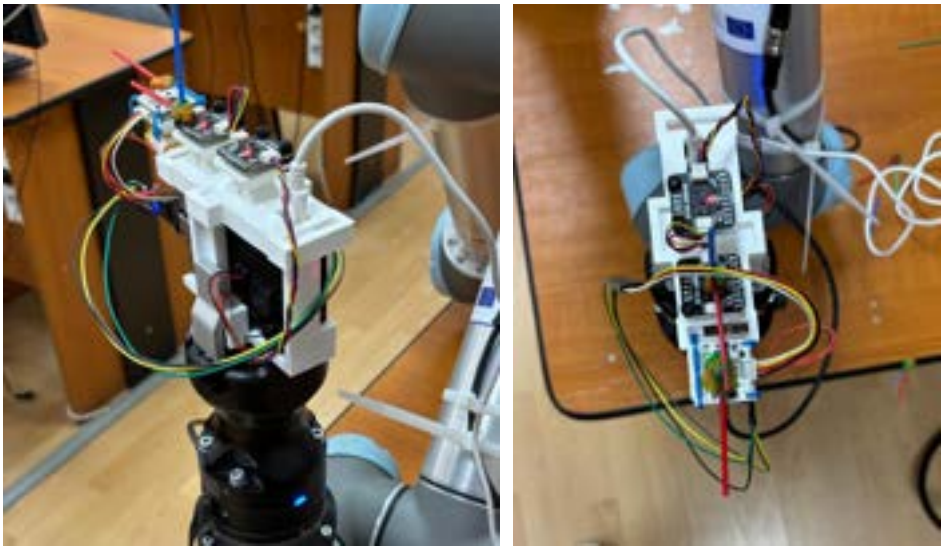


Figure 5: RaspberryPI with IMU sensors on UR5 arm. Left: Side view. Right: top view.

With the data gathered, an EKF is run either with one or both IMUs. Note that only using IMU accelerations, without either velocity and position feedback, the position estimate would be divergent. To get useful data, we, therefore, also include absolute position data from the end-effector but corrupted by noise and read only once every second.

### 3.3 Smart Grapple System

As shown in Fig. 6, the USG is a Unmanned Underwater Vehicle (UUV) connected by a tether to the USV. This USG can be driven by the thrusters equipped on itself and by the pulling or releasing of the tether driven by the USV, where the tether is fixed on the winch. The states of the USG system are collected in the vector below:

$$\boldsymbol{x} = [x, d, X, \theta, r, \dot{x}, \dot{d}, \dot{X}, \dot{\theta}, \dot{r}]^T \tag{26}$$

Similarly to the previous section, the position of UUV $[x, d]^T$ can be measured by the sensors SBL, USBL, UAV camera, and camera laced on the shore, and the USV position $X$ is determined by the GPS. The velocities of UUV $[\dot{x}, \dot{d}]^T$ and USV $\dot{X}$ are measured by DVL, and the angular position as well as velocity of UUV $\theta, \dot{\theta}$ are measured by IMU. The motion between USV and UUV $r, \dot{r}$ can be calculated by the positions and the velocities of UUV and USV. Based on the following derivation

- The relationship between USV and UUV is derived as $x = X - r\sin(\theta), d = r\cos(\theta)$
- The system states $x$ as well as $d$ can be represented as $r, \theta$

Co-funded by the European Union

SeaClear2.0 is co-funded by the European Union under the Horizon Europe Programme (Grant Agreement 101093822). Views and opinions expressed herein are those of the author(s) and do not necessarily reflect those of the European Union or European Climate, Infrastructure and Environment Executive Agency (CINEA). Neither the European Union nor the granting authority can be held responsible for them

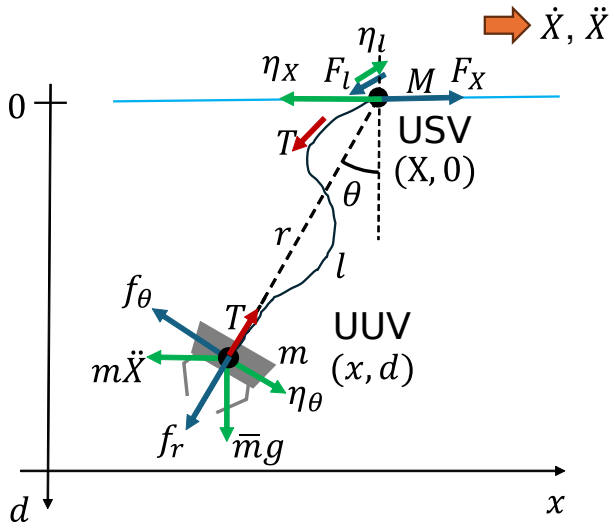



Figure 6: This figure illustrates the setting of our smart grapple system in 2D plane. The sea surface is represented by $d = 0$, where the USV is located. The force effect on USV and UUV, which are connected by the tether, are introduced in this figure.

- The tether length is written as $l$

the simplified system states are written as

$$\boldsymbol{q} = [\theta, r, l, X]^T \tag{27}$$

With the following assumptions

- The inertia and the gravity of the tether can be ignored in the underwater environment,
- The environmental effect on the USG are negligible compared to the forces produced by the thrusters or the tether,

the system dynamics is formulated as a hybrid system with two modes. The first mode describes the dynamics when there is zero tension force on the tether:

**Mode I ($T = 0$)**

$$\begin{cases} M\ddot{X} = -\eta_X(\dot{X}) + F_X \\ mr^2\ddot{\theta} = m\ddot{X}r\cos\theta - 2mr\dot{r}\dot{\theta} - \bar{m}gr\sin\theta \\ \qquad\quad +r(-\eta_\theta(\dot{\theta}, \dot{X}) + f_\theta) \\ m\ddot{r} = m\ddot{X}\sin\theta + mr\dot{\theta}^2 + \bar{m}g\cos\theta - \eta_r(\dot{r}, \dot{X}) + f_r \\ I_l\ddot{l} = -\eta_l(\dot{l}) + F_l \end{cases} \tag{28}$$

and the second mode formulates the case when there is a non-negligible tension force on the tether:


Co-funded by the European Union

SeaClear2.0 is co-funded by the European Union under the Horizon Europe Programme (Grant Agreement 101093822). Views and opinions expressed herein are those of the author(s) and do not necessarily reflect those of the European Union or European Climate, Infrastructure and Environment Executive Agency (CINEA). Neither the European Union nor the granting authority can be held responsible for them

**Mode II ($T > 0$)**

$$\begin{cases} M\ddot{X} = -\eta_X(\dot{X}) + F_X \\ mr^2\ddot{\theta} = m\ddot{X}r\cos\theta - 2mr\dot{r}\dot{\theta} - \bar{m}gr\sin\theta \\ \qquad\qquad + r(-\eta_\theta(\dot{\theta}, \dot{X}) + f_\theta) \\ (m + I_l)\ddot{r} = m\ddot{X}\sin\theta + mr\dot{\theta}^2 + \bar{m}g\cos\theta \\ \qquad\qquad - \eta_r(\dot{r}, \dot{X}) - \eta_l(\dot{r}) + f_r + F_l \\ \ddot{l} = \ddot{r} \end{cases} \tag{29}$$

where the dynamic parameters are formulated as follows

- Mass: $M$(USV), $m$(UUV), $\bar{m}$(collected litter)
- Force: $F_X$(thruster force on USV), $F_l$(winch on USV), $f_\theta$, $f_r$(thruster force on UUV)
- Drag force: $\eta_X$(USV), $\eta_l$(winch on USV), $\eta_\theta, \eta_r$(UUV)
- Inertia: $I_l$(winch on USV)

We consider the predominant motion of the grapple to be in the longitudinal $x$ and the surge direction of the USV $d$ and, therefore, disregard the motion in the sway direction.

This is trivial to extend to a full 3D system.

To consider the more complicated behavior of the USG, we derive the dynamics of the system with the tether under tension in the following. The state space representation of (28) is written as follows

$$M(\boldsymbol{q})\ddot{\boldsymbol{q}} = k(\boldsymbol{q}, \dot{\boldsymbol{q}}) + B(\boldsymbol{q})\boldsymbol{f} \tag{30}$$

where $\boldsymbol{q} = [\theta, r, l, X]^T$, $\boldsymbol{f} = [f_\theta, f_r, F_l, F_X]^T$, and $M(\boldsymbol{q}), k(\boldsymbol{q}, \dot{\boldsymbol{q}}), B(\boldsymbol{q})$ are represented as

$$M(\boldsymbol{q}) = \begin{pmatrix} mr^2 & 0 & 0 & -mr\cos\theta \\ 0 & m + I_l & 0 & -m\sin\theta \\ 0 & -1 & 1 & 0 \\ 0 & 0 & 0 & M \end{pmatrix} \tag{31}$$

$$k(\boldsymbol{q}, \dot{\boldsymbol{q}}) = \begin{pmatrix} -2mr\dot{r}\dot{\theta} - \bar{m}gr\sin\theta - r\eta_\theta \\ mr\dot{\theta}^2 + \bar{m}g\cos\theta - \eta_r - \eta_l \\ 0 \\ -\eta_X \end{pmatrix} \tag{32}$$

$$B(\boldsymbol{q}) = \begin{pmatrix} r & 0 & 0 & 0 \\ 0 & 1 & 1 & 0 \\ 0 & 0 & 0 & 0 \\ 0 & 0 & 0 & 1 \end{pmatrix} \tag{33}$$

Co-funded by the European Union

SeaClear2.0 is co-funded by the European Union under the Horizon Europe Programme (Grant Agreement 101093822). Views and opinions expressed herein are those of the author(s) and do not necessarily reflect those of the European Union or European Climate, Infrastructure and Environment Executive Agency (CINEA). Neither the European Union nor the granting authority can be held responsible for them

# 4 Pose Estimation Results

This section describes experiments and evaluations of the pose estimation filters implemented for the various SeaClear2.0 systems. Note that while the basic filter structure and algorithmic implementation are shared among the systems, the individual motion models and different sensors require individual tuning and lead to differing results in coping with the pose estimation uncertainties.

## 4.1 USV Pose Estimation

In this subsection, we will outline the experimental setup and results of the USV pose estimation trials. We will discuss the methodologies used, the performance of the pose estimation algorithms, and the implications for reliable USV navigation. The following sections will provide insights into the effectiveness of the integrated systems and propose potential enhancements.

### 4.1.1 Experimental setup and preliminaries

The experimental data was acquired during sea trials that have taken place in the week 23-27/09/2024 on the Lake Schlei ($54°29'52.5"$N, $9°40'31.3"$E), in the state of Schleswig-Holstein, Germany. The tests were conducted using Fraunhofer CMLs SeaDragon USV, depicted in Figure 7 operated using course and speed controllers.



Figure 7: SeaDragon USV, shuttle tender USV used in SeaClear2.0 (without litter storage mounted)

Co-funded by the European Union

SeaClear2.0 is co-funded by the European Union under the Horizon Europe Programme (Grant Agreement 101093822). Views and opinions expressed herein are those of the author(s) and do not necessarily reflect those of the European Union or European Climate, Infrastructure and Environment Executive Agency (CINEA). Neither the European Union nor the granting authority can be held responsible for them

As mentioned in Section 3.1, the kinematics of the USV in the local horizontal plane are described by the velocity vector $\mathbf{v} = [u, v, r]^\top$, while the pose vector $\boldsymbol{\eta} = [x, y, \psi]^\top$ includes the pose and heading angle of the vessel. The pose, heading angle and velocities are computed by an EKF on-board of the Xsens Inertial Navigation Systems (INS). In addition, a separate measurement, using solely Global Navigation Satellite System (GNSS) data, was available during sea trials. The latter is used as a reference for comparing the performance of the pose estimation of the vessel. As seen in Figure 8, the reference point for the Xsens INS is the midpoint of the mast, while the Septentrio GNSS receiver refers all measurements to the starboard (#1) antenna.

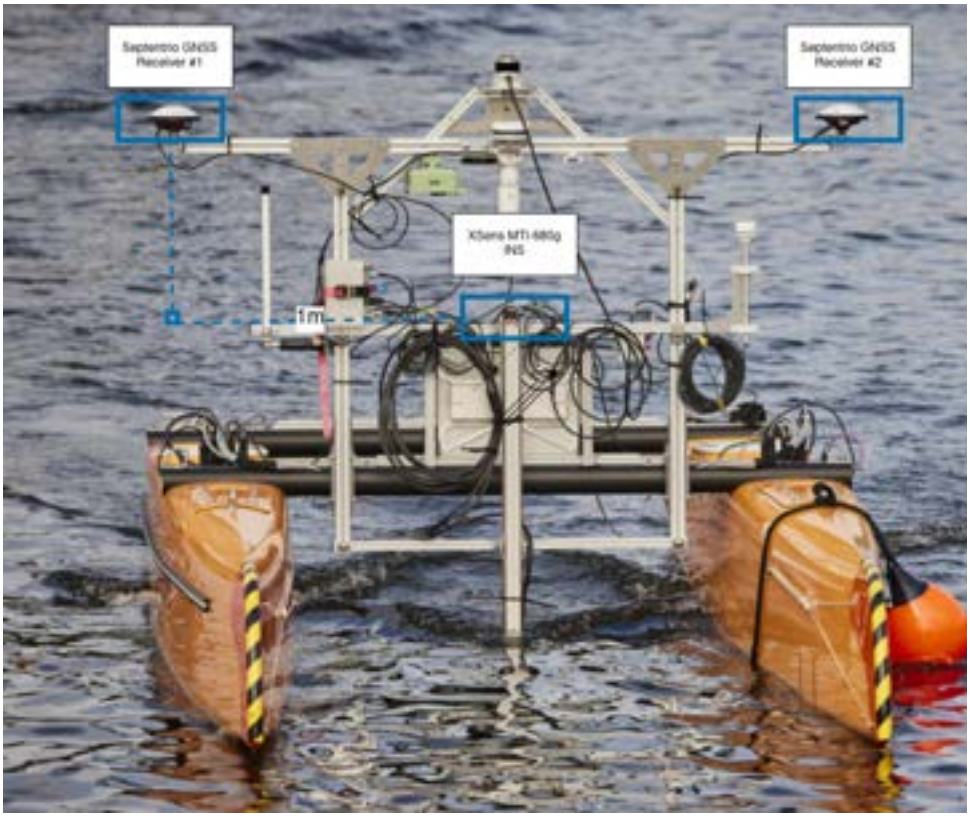



Figure 8: Layout of the two GNSS antenna's onboard SeaDragon USV

The independent measurement uses a Septentrio dual-head GNSS receiver, enhanced with ground-based augmentation system (GBAS) and Real-Time Kinematics (RTK) reference stations. As shown in Figure 9, provided that the baseline used for augmentation or corrections are within close area, the accuracy of the GBAS-enhanced GNSS should be under $1\,\mathrm{m}$.

For comparing the vehicle poses, the $[x, y]^\top$ positions are obtained by converting the coordinates into North-East-Down (NED) frame. The yaw angle $\psi$ is obtained from the INS orientation vector, while the Septentrio GNSS makes uses of the dual-antenna for differentially calculate the heading angle. The velocity readings are not compared directly, as solely a course and speed controller has been used, but rather integrated into the course angle. Hence, the evaluated readings comprise solely $[u, v]^\top$.

The *course angle* $\chi$ represents the direction of the vehicle's velocity vector relative to the North-East

[3] https://gssc.esa.int/navipedia/index.php/GNSS_Augmentation

Co-funded by the European Union

SeaClear2.0 is co-funded by the European Union under the Horizon Europe Programme (Grant Agreement 101093822). Views and opinions expressed herein are those of the author(s) and do not necessarily reflect those of the European Union or European Climate, Infrastructure and Environment Executive Agency (CINEA). Neither the European Union nor the granting authority can be held responsible for them

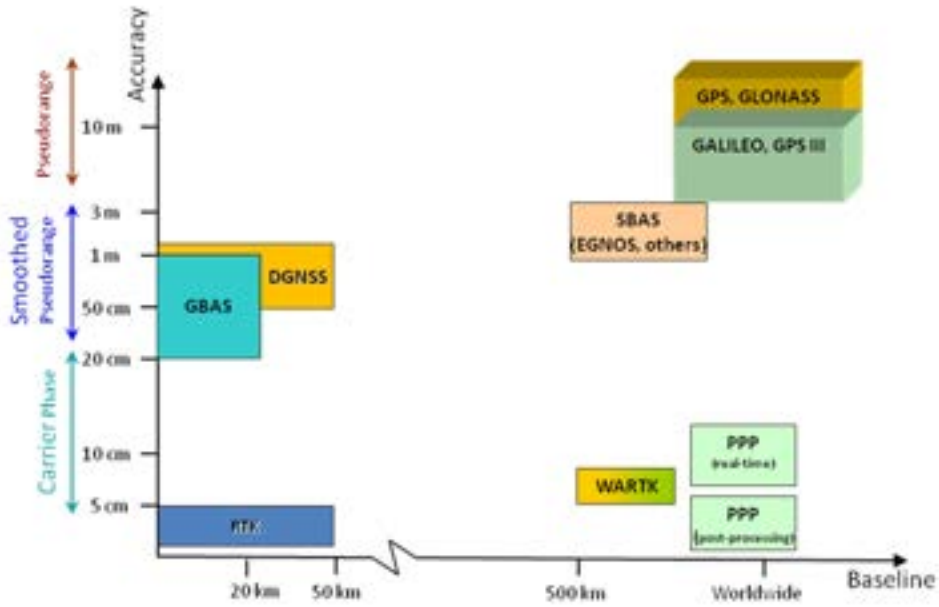



Figure 9: Classification of GNSS accuracy based on augmentation information coming from satellites[3]

frame. It is calculated as the sum of the heading angle $\psi$ (from the compass) and the *crab angle* $\beta$, which accounts for the drift caused by sway ($v$) and surge ($u$) velocities in the body frame. Using Fossen's notation [4], the crab angle is given by:

$$\beta = \tan^{-1}\left(\frac{v}{u}\right).$$

The course angle is then calculated as:

$$\chi = \psi + \beta = \psi + \tan^{-1}\left(\frac{v}{u}\right).$$

Here, $u$ and $v$ are the velocities along the $x$ (surge) and $y$ (sway) axes in the body-fixed frame, respectively. The crab angle $\beta$ ensures the course accounts for drift caused by environmental forces such as currents and wind.

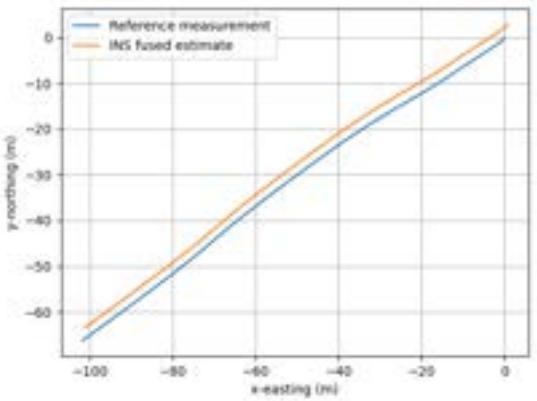
The quality of the global position estimation of the GNSS is highly impacted by the of satellite geometry. Dilution of Precision (DOP) metrics assess these errors, by encompassing positional and time-related errors. During the sea trials the median values of DOP measurands have been:

- Geometric Dilution of Precision (GDOP) = 1.4
- Position Dilution of Precision (PDOP) = 1.3
- Vertical Dilution of Precision (VDOP) = 0.9
- Horizontal Dilution of Precision (HDOP) = 0.7

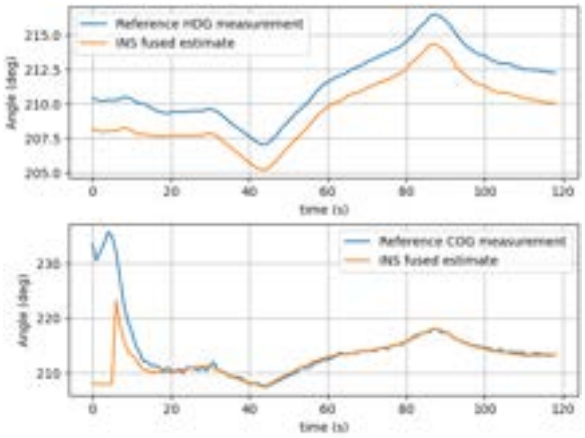
These values suggest a strong satellite geometry, implying reliable GNSS positional accuracy. Typically, DOP values below 2 are considered excellent [9], indicating minimal geometric dilution and high confidence in the positional data.

Co-funded by the European Union

SeaClear2.0 is co-funded by the European Union under the Horizon Europe Programme (Grant Agreement 101093822). Views and opinions expressed herein are those of the author(s) and do not necessarily reflect those of the European Union or European Climate, Infrastructure and Environment Executive Agency (CINEA). Neither the European Union nor the granting authority can be held responsible for them




(a) The position readings of the SeaDragon USV




(b) The heading (up) and course (down) readings comparison

Figure 10: Trial 1: SeaDragon USV pose estimation in a simple scenario, following a constant course and speed

### 4.1.2 Results

The results have been compared in 5 trials by averaging the errors obtained by comparing the pose and velocity readings obtained with the two systems, within an interval of $25\ \mathrm{ms}$. The reference GNSS system operated at a frequency of $2\ \mathrm{Hz}$, while the Xsens INS operated at $100\ \mathrm{Hz}$. The sampling frequency used was $2\ \mathrm{Hz}$. The errors are summarised in Table 2.

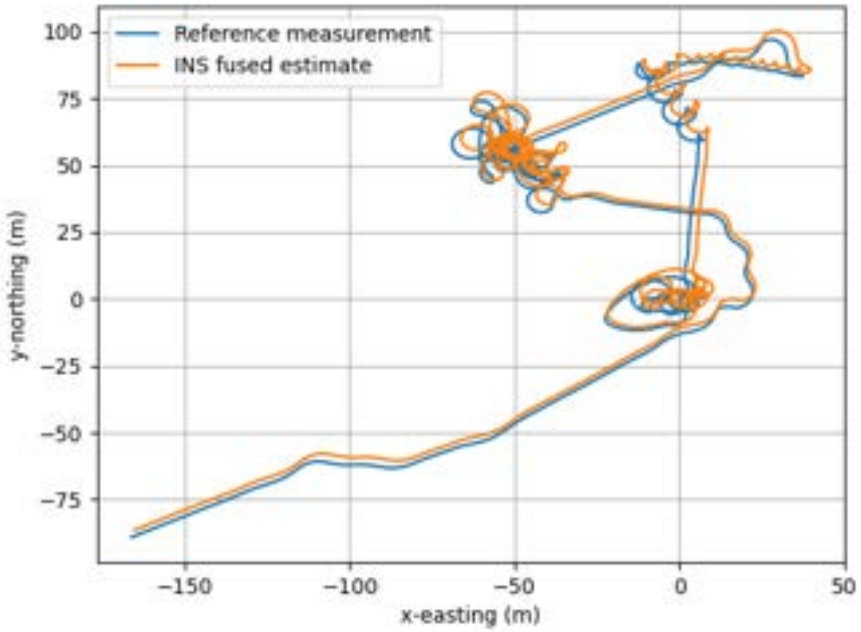
In Trial 1, constant course and speed are sought by the vehicle. As it can be seen in Figure 10, the pose errors are rather constant, while the course errors present some slight differences at the beginning, likely due to the vehicle's acceleration.

In a more complex scenario, Trial 4, the vehicle is commissioned to follow various courses and speeds within specific time intervals and within a small operation area. The purpose of this scenario is to replicate the common use-case for the shuttle tender USV within SeaClear2.0: periods of constant course and speed navigation are expected when navigating to the target USV position. These are followed by multiple changes of course within a short time, specific to the manoeuvres found in confined spaces, like harbours, or to station-keeping relative to the SeaCAT2 for litter transfer. As expected, the greatest impact in terms of performances is on the velocities, which generated jerky readings of the course angle, as depicted in Figure 11.

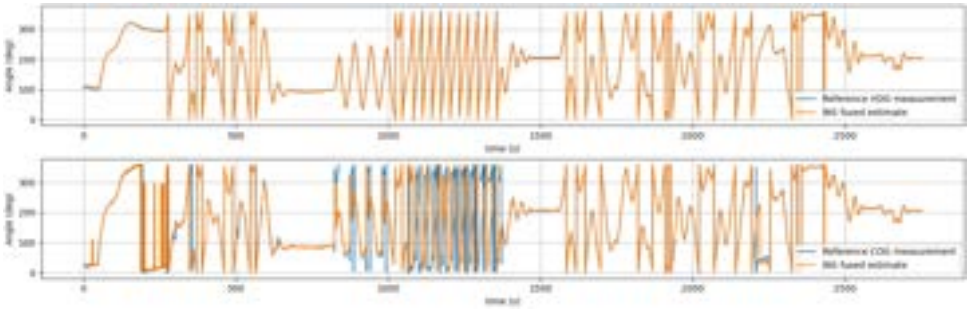
The pose estimation given by the INS on-board SeaDragon USV has shown overall good performance when compared with the chosen baseline. The most critical moment of the operation of the SeaDragon USV as a shuttle tender, is the approach for docking on the SeaCat2 USV. For this, a separate pipeline for computing the relative pose will be used, thus augmenting the current pose estimation algorithm. For example, visual perception (both camera- and Light Detection and Ranging (LiDAR)-based) may be used in that setting.


Co-funded by the European Union

SeaClear2.0 is co-funded by the European Union under the Horizon Europe Programme (Grant Agreement 101093822). Views and opinions expressed herein are those of the author(s) and do not necessarily reflect those of the European Union or European Climate, Infrastructure and Environment Executive Agency (CINEA). Neither the European Union nor the granting authority can be held responsible for them




(a) The position readings of the SeaDragon USV



(b) The heading (up) and course (down) readings comparison

Figure 11: Trial 4: SeaDragon USV pose estimation in a more complex scenario, with periods of abrupt course change


Co-funded by the European Union

SeaClear2.0 is co-funded by the European Union under the Horizon Europe Programme (Grant Agreement 101093822). Views and opinions expressed herein are those of the author(s) and do not necessarily reflect those of the European Union or European Climate, Infrastructure and Environment Executive Agency (CINEA). Neither the European Union nor the granting authority can be held responsible for them

Table 2: Overview of the average positional and orientation errors acquired during 5 different trials

| | Distance [m] | Pose error [m] | Orientation error [deg] | Course error [deg] |
|---|---|---|---|---|
| Trial 1 | 121.55 | 1.89 | 1.99 | 1.85 |
| Trial 2 | 258.84 | 0.91 | 3.29 | 1.23 |
| Trial 3 | 380.5 | 1.77 | 2.08 | 10.78 |
| Trial 4 | 1312.59 | 1.86 | 2.16 | 14.83 |
| Trial 5 | 1585.26 | 0.54 | 1.93 | 3.45 |

## 4.2 ROV Pose Estimation

We begin with a set of main results where the linear accelerations of the IMU are not used. Then, we attempt to use these accelerations.

### 4.2.1 Main results



Figure 12: UTC team running pose estimation experiments in Marseille. The ROV is underwater, and the pole with the shore camera is visible on the right side of the figure.

MiniTortuga experiments were run in October 2024 in Marseille, France (see Figure 12), with the full sensor suite described in Section 3.2 except the UAV camera. Both the SBL and USBL base stations were mounted near the quay. The goal of the experiments was threefold:


Co-funded by the European Union

SeaClear2.0 is co-funded by the European Union under the Horizon Europe Programme (Grant Agreement 101093822). Views and opinions expressed herein are those of the author(s) and do not necessarily reflect those of the European Union or European Climate, Infrastructure and Environment Executive Agency (CINEA). Neither the European Union nor the granting authority can be held responsible for them

1. Validate the pose estimation pipeline for underwater vehicles.
2. Determine which of the two acoustic positioning sensors (SBL, USBL) provides better performance.
3. With the selected sensor, determine the position estimation error of the ROV.

To address Objective 1, we perform – among many other experiments – a manually-controlled, roughly 12-minute long ROV trajectory and record its position as measured by the (a) shore camera, (b) SBL, (c) USBL, and (d) Doppler Velocity Logger (DVL)-based dead reckoning. Case (d) sets the absolute position manually at the start of the trajectory, and afterwards runs the EKF using only the onboard sensors. The position is stable enough to be compared to the other sensors. Results are shown in Figure 13. Note that the signal from (a) the shore camera is only available when the ROV is in the camera frame. All scenarios largely agree with each other with the exception of (c) where the USBL is used, which has relatively large deviations. Numerically, taking the shore-cam as a reference position (approximation of the ground truth), the average position errors across the time interval where the shore camera sees the ROV are:

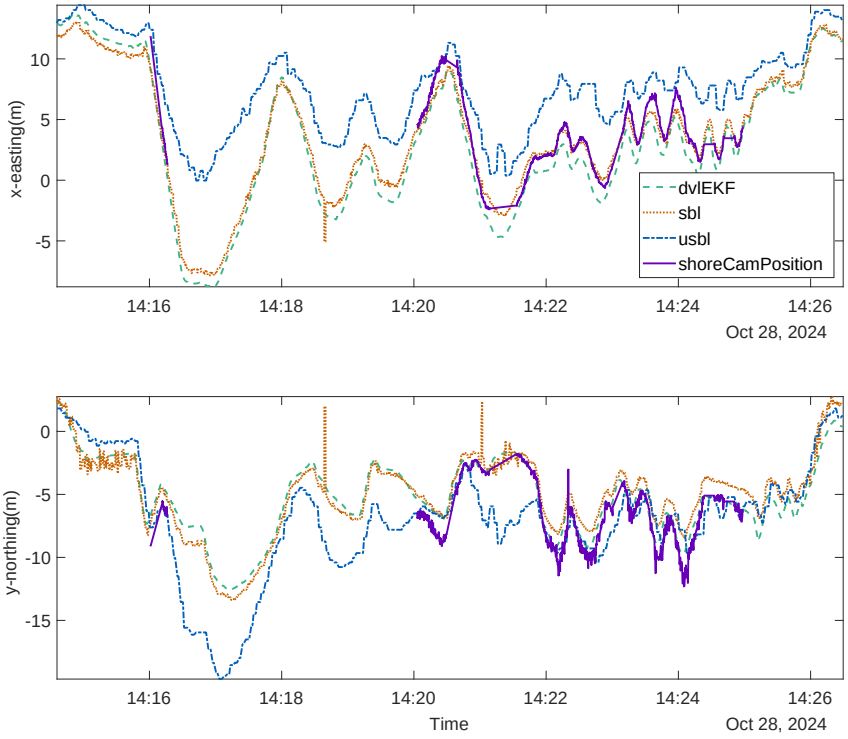



Figure 13: Comparison between MiniTortuga positions estimated using several sensor configurations. Separate X and Y coordinates. The shore-camera measurement is only plotted for the duration of time when it is available.

To investigate more deeply the USBL performance, we also plot the trajectory in the plane, in a different experiment in which the ROV was performing a rectangular trajectory. Here we only compare setups (b), (c), and (d). The results in Figure 14 show that the USBL measurements become increasingly rotated

Co-funded by the European Union

SeaClear2.0 is co-funded by the European Union under the Horizon Europe Programme (Grant Agreement 101093822). Views and opinions expressed herein are those of the author(s) and do not necessarily reflect those of the European Union or European Climate, Infrastructure and Environment Executive Agency (CINEA). Neither the European Union nor the granting authority can be held responsible for them

as the ROV moves further away from the base station.[4] Our conclusion is that USBL is not reliable within our scenario; the reasons for this behavior will be investigated further in subsequent experiments and pilots. One possible reason is that the shallow water in which we performed the experiments in Marseille leads to suboptimal USBL performance.

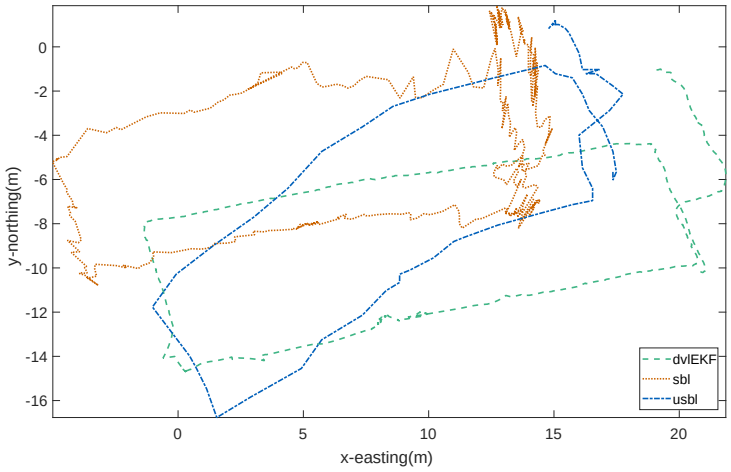



Figure 14: Comparison between MiniTortuga positions estimated using several sensor configurations. Position trajectory in the plane.

To address Objective 2, for the time interval in Figure 13 where the ROV was seen by the shore camera, we rerun the EKF but now including the SBL measurements in addition to the onboard sensors, leading to a full set of sensors. The position from the shore camera is again treated as a reference. The results are given in Figure 15. The mean error between the camera-based reference and the positions as estimated by the EKF is $1.7$ m. This is still too large to fully achieve our mapping Key Performance Indicators (KPIs), so we will work to reduce it in future experiments and pilots. One direction will be to test USBL accuracy in deeper water, with the beacon mounted on the SeaCat2. Another is to use, like in SeaClear, intermittent position measurements using the UAV camera, by periodically resurfacing the ROV.

Note that while in these figures we focus on the ROV position in the plane because it is the only signal for which we can obtain a reliable reference value, the EKF estimate, of course, also includes the depth and attitude of the ROV. In SeaClear we already indirectly validated these signals via good mapping results.

### 4.2.2 Results using acceleration measurements from the IMU

Figure 16 shows the pose estimation results obtained with the EKF using **the state vector that includes biases**, shown in (22), compared to EKF with the basic kinematic model used so far. Neither estimate uses any absolute measurement source. Recall that a main feature of the model with state (22) is that linear acceleration measurements are used. Overall, despite the attempt of the new filter to compensate biases, linear accelerations are still too noisy and they introduce large errors.

[4] Note that in these results the DVL-based trajectory has an offset compared to the other two sensors, likely because the initial, manually-input position included this offset.

Co-funded by the European Union

SeaClear2.0 is co-funded by the European Union under the Horizon Europe Programme (Grant Agreement 101093822). Views and opinions expressed herein are those of the author(s) and do not necessarily reflect those of the European Union or European Climate, Infrastructure and Environment Executive Agency (CINEA). Neither the European Union nor the granting authority can be held responsible for them

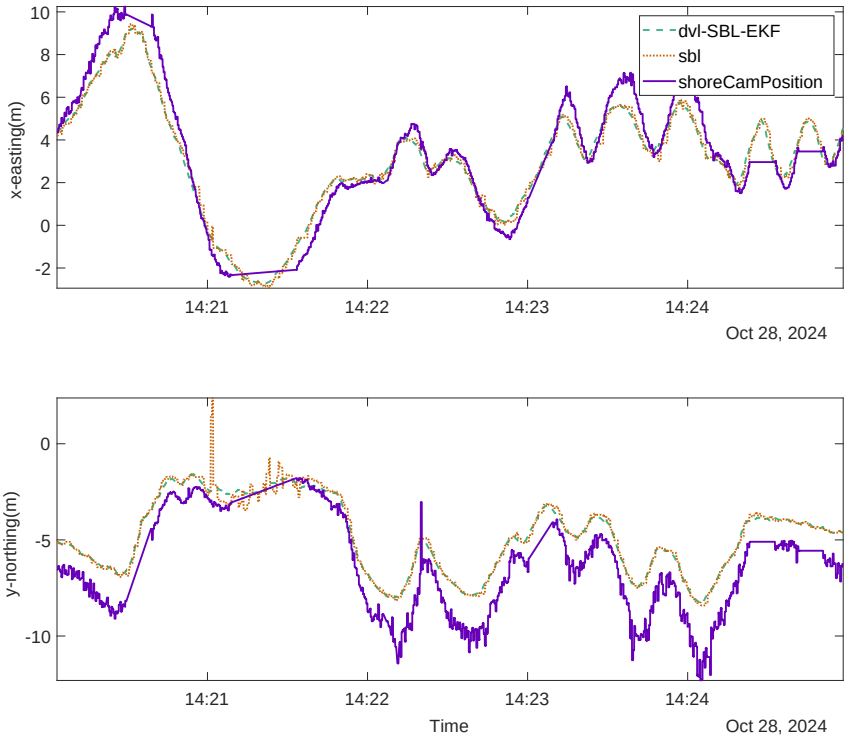



Figure 15: MiniTortuga pose estimation experiment, with the shore-camera position used as a reference. The SBL position (uncorrected by DVL and IMU) is also recorded.

Figure 17 shows the results of running the **multi-IMU experiment** described in Section 3.2.3. With either one or two IMUs, the filter follows the position measurements, but large deviations are significantly rarer when two IMUs are used. Note that we ran multiple experiments and this result is representative (although in certain experiments, due to lucky noise realizations, the one-IMU setup may work better). This shows that using two IMUs has the potential to improve the quality of a position estimate. However, there are still large error spikes caused by double-integrating biased and noisy accelerations.

Overall, it seems that the large amount of noise in the linear acceleration measurements makes it so that adding this information to the overall ROV filter will not lead to better results than simply using the linear velocities measured by the DVL. Therefore, while we will still investigate solutions to this issue, it is unlikely that linear accelerations will be used in the pose estimator.


Co-funded by the European Union

SeaClear2.0 is co-funded by the European Union under the Horizon Europe Programme (Grant Agreement 101093822). Views and opinions expressed herein are those of the author(s) and do not necessarily reflect those of the European Union or European Climate, Infrastructure and Environment Executive Agency (CINEA). Neither the European Union nor the granting authority can be held responsible for them

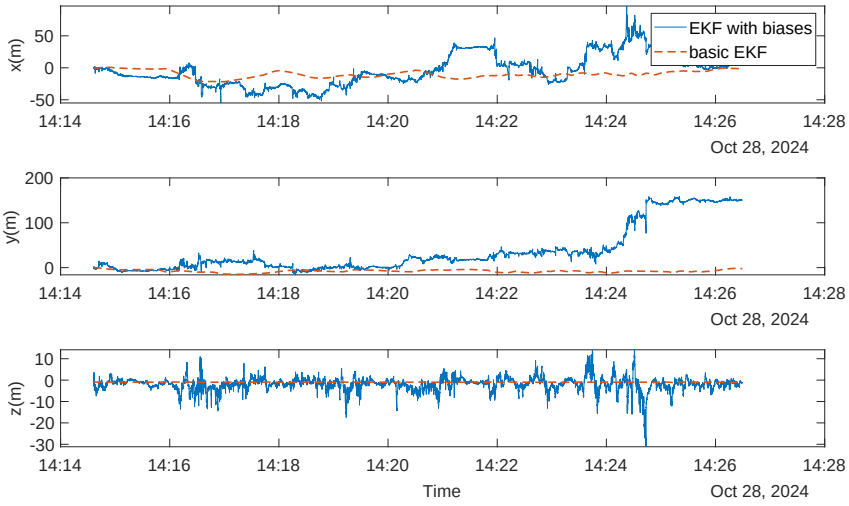



Figure 16: MiniTortuga pose estimation test for the new model that includes bias estimates and linear accelerations.

### 4.3 Simulated Pose Estimation Results for the Smart Grapple

We evaluated the pose estimation functionalities for the smart grapple within the highly realistic MArine Robotic Unity Simulator (MARUS) simulation [10]. A visualization of the different blocks involved in the pose estimation is shown in Fig. 18. While the EKF block relies on the *robot_localization* package [11], the remaining functionalities have been adapted from Seaclear1.0, migrated from Robot Operating System (ROS)1 to ROS2, and deployed to work with the Unity sensors.

The primary goal of this section is to verify that the pose estimation node integrates correctly with the grapple rather than evaluating the accuracy or reliability of different sensor fusion strategies at this stage. We opted for this approach to be able to perform simulated tests during the development of the smart grapple hardware, which was integrated at the end of 2024. Note that we expect the experimental findings for the Mini Tortuga to be fully transferrable to the smart grapple pose estimation. As to be seen in Fig. 18, we fused the following sensor measurements in the EKF:

- IMU: Angular positions $\phi, \theta, \psi$, Angular velocities $\dot{\phi}, \dot{\theta}, \dot{\psi}$.
- DVL: Linear velocities $v_x, v_y, v_z$.
- Global Positioning System (GPS): Linear positions $x, y, z$.

Although the IMU also provides linear acceleration measurements, they are excluded due to their unreliability, as observed in Section 4.2. It is important to note that directly using the Unity GPS sensor within the EKF, rather than employing a combination of SBL and a pressure sensor, can lead to overly optimistic results. Therefore, to introduce realism and challenge the pose estimation system, we artificially add noise to the measurements, see Table 3.

Figure 19 presents an example trajectory along with the position tracking output from the state estimation compared to the ground truth positions provided by MARUS.

Co-funded by the European Union

SeaClear2.0 is co-funded by the European Union under the Horizon Europe Programme (Grant Agreement 101093822). Views and opinions expressed herein are those of the author(s) and do not necessarily reflect those of the European Union or European Climate, Infrastructure and Environment Executive Agency (CINEA). Neither the European Union nor the granting authority can be held responsible for them

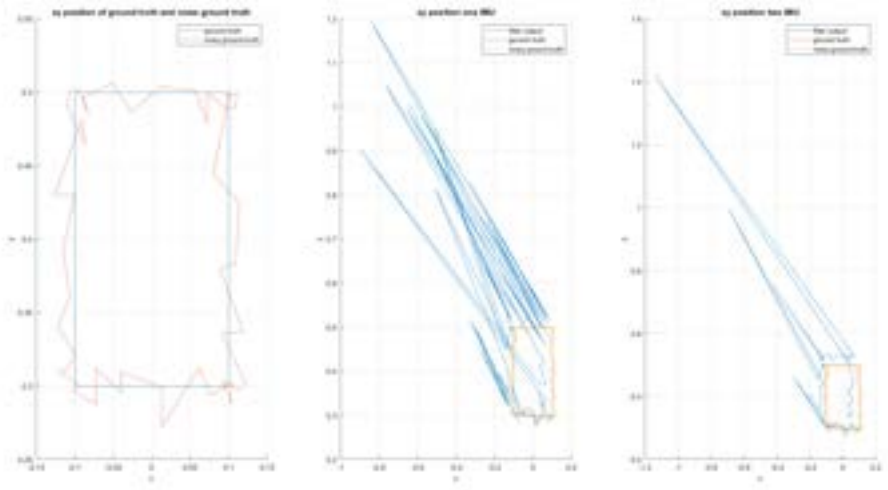


Figure 17: Comparison between using one and two IMUs. Left: end-effector positions together with their artificially noise-corrupted versions used in the estimator. Middle: estimated position using only one IMU. Right: Estimated position using two IMUs.

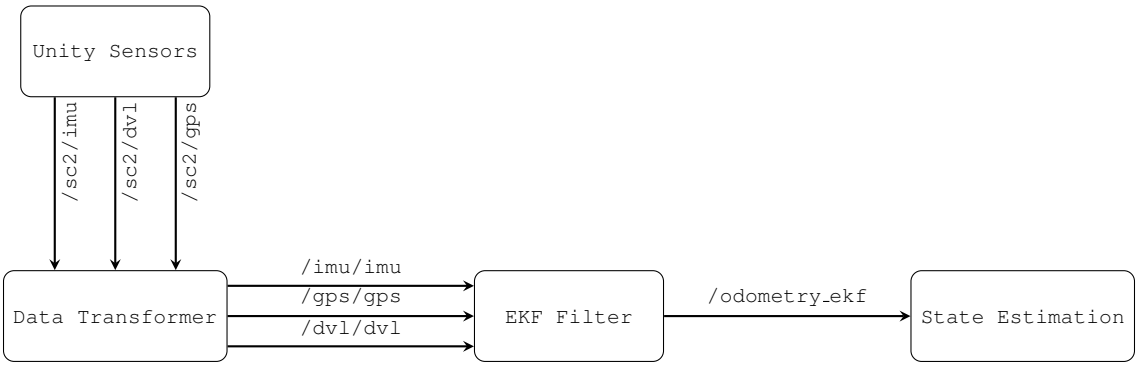



Figure 18: ROS2 Software Architecture for the State Estimation

To quantify the pose estimation accuracy, we compute the Root Mean Square Error (RMSE) for the $x$, $y$, and $z$ components of the trajectory. For example, the RMSE for the $x$ component is given by $\mathrm{RMSE}_x = \sqrt{\frac{1}{N}\sum_k (\hat{x}_n - x_{n,\mathrm{grapple}})^2}$, where $N$ is the number of measurements, and $\hat{x}$ represents the estimated $x$-position from the EKF. The computed RMSE values for the three spatial components yields $\mathrm{RMSE}_{x,y,z} = \begin{bmatrix} 0.035 & 0.036 & 0.038 \end{bmatrix}$.

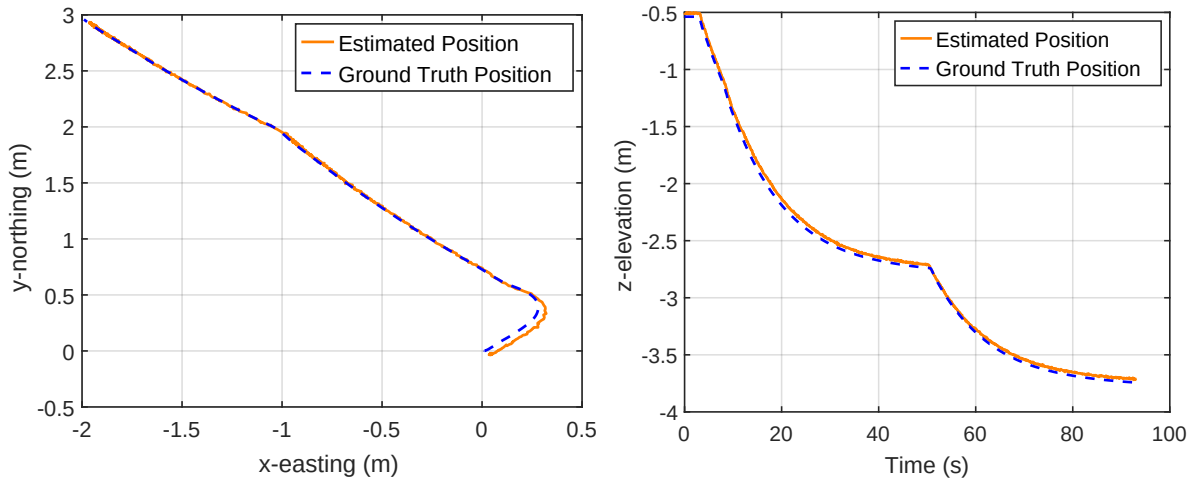
These results could be further improved by the integration of a pressure sensor into the EKF, which provides a highly reliable depth measurement, and by incorporating the SeaCat2 USV into the MARUS simulation. This will enable us to evaluate the state estimation module in a more realistic scenario using SBL or USBL sensor data before validating it through hardware experiments in the upcoming pilot test.

Co-funded by the European Union

SeaClear2.0 is co-funded by the European Union under the Horizon Europe Programme (Grant Agreement 101093822). Views and opinions expressed herein are those of the author(s) and do not necessarily reflect those of the European Union or European Climate, Infrastructure and Environment Executive Agency (CINEA). Neither the European Union nor the granting authority can be held responsible for them

| | GPS | IMU | |
|---|---|---|---|
| | | Gyro | Orientation |
| Bias | 0.03 | 0.01 | 0.01 |
| Std | 0.01 | 0.01 | 0.01 |

Table 3: Bias and standard deviation for GPS and IMU sensors




(a) Position trajectory in the $x - y$ plane

(b) Corresponding elevation trajectory

Figure 19: Grapple Pose Estimation Results. EKF fusing GPS, IMU and DVL compared to the ground truth read from the MARUS simulation block [10].


Co-funded by the European Union

SeaClear2.0 is co-funded by the European Union under the Horizon Europe Programme (Grant Agreement 101093822). Views and opinions expressed herein are those of the author(s) and do not necessarily reflect those of the European Union or European Climate, Infrastructure and Environment Executive Agency (CINEA). Neither the European Union nor the granting authority can be held responsible for them

# 5 Conclusions

This report has presented the methodologies and advancements in pose estimation techniques for the SeaClear 2.0 project, focusing on Unmanned Surface Vehicles (USVs), Remotely Operated Vehicles (ROVs), and the Smart Grapple system. The integration of sensor fusion techniques, particularly the Extended Kalman Filter (EKF), has been central to improving the accuracy and reliability of pose estimation across these marine robotic platforms.

Experimental results indicate the effectiveness of the proposed techniques in practical scenarios. The MiniTortuga ROV experiments demonstrated that the Short Baseline (SBL) sensor outperforms the Ultra-Short Baseline (USBL) sensor in terms of position accuracy. Additionally, the use of multiple Inertial Measurement Units (IMUs) showed potential for enhancing pose estimation accuracy, although the noise and biases in linear acceleration measurements remain a challenge.

For the SeaDragon USV, the pose estimation system performed robustly during sea trials. The onboard Inertial Navigation System (INS) provided reliable data when compared to the reference Global Navigation Satellite System (GNSS). The integration of visual perception techniques, such as camera and LiDAR-based corrections, is anticipated to further improve the accuracy of the USV's pose estimation, especially during docking maneuvers.

Simulated tests for the Smart Grapple system within the MARUS simulation environment yielded promising results. The EKF effectively fused data from simulated GPS, IMU, and Doppler Velocity Logger (DVL) sensors. Future work will focus on integrating additional sensors, such as pressure sensors, and conducting hardware experiments to validate the simulation findings.

In summary, the advancements in pose estimation techniques detailed in this report provide a solid foundation for the continued development and deployment of autonomous robotic systems in general, and of the SeaClear2.0 system for marine litter collection in particular.

Co-funded by the European Union

SeaClear2.0 is co-funded by the European Union under the Horizon Europe Programme (Grant Agreement 101093822). Views and opinions expressed herein are those of the author(s) and do not necessarily reflect those of the European Union or European Climate, Infrastructure and Environment Executive Agency (CINEA). Neither the European Union nor the granting authority can be held responsible for them

## References

[1] K. D. Do and J. Pan, *Control of Ships and Underwater Vehicles*, ser. Advances in Industrial Control. Springer London, 2009. [Online]. Available: http://link.springer.com/10.1007/978-1-84882-730-1

[2] Society of Naval Architects and Marine Engineers (U.S.), Technical and Research Committee, Hydrodynamics Subcommittee, *Nomenclature for Treating the Motion of a Submerged Body Through a Fluid: Report of the American Towing Tank Conference*, ser. Technical and research bulletin. Society of Naval Architects and Marine Engineers, 1950. [Online]. Available: https://books.google.de/books?id=VqNFGwAACAAJ

[3] R. Skjetne, O. Smogeli, and T. Fossen, "A nonlinear ship manoeuvering model: Identification and adaptive control with experiments for a model ship," *Modeling, Identification and Control*, vol. 25, pp. 3–27, 2004.

[4] T. I. Fossen, *Handbook of Marine Craft Hydrodynamics and Motion Control*, 2nd ed. Wiley, 2021.

[5] ——, *Marine control systems - Guidance. navigation, and control of ships, rigs and underwater vehicles*, 2002.

[6] Mathworks. Estimate pose from MARG and GPS data. [Online]. Available: https://www.mathworks.com/help/nav/ref/insfiltermarg.html

[7] R. Friedberg, "Rodrigues, olinde: "des lois géométriques qui régissent les déplacements d'un système solide...", translation and commentary," 2022. [Online]. Available: https://arxiv.org/abs/2211.07787

[8] T. Alinei-Poiană, D. Reţe, D. Martinovici, V.-M. Maer, and L. Buşoniu, "A BlueROV2-based platform for underwater mapping experiments," *IFAC-PapersOnLine*, vol. 58, no. 20, pp. 470–475, 2024.

[9] M. Tahsin, S. Sultana, T. Reza, and M. Hossam-E-Haider, "Analysis of DOP and its preciseness in GNSS position estimation," in *2015 International Conference on Electrical Engineering and Information Communication Technology (ICEEICT)*, 2015, pp. 1–6.

[10] I. Loncar, J. Obradovic, N. Kraševac, L. Mandić, I. Kvasić, F. Ferreira, V. Slosic, Đula Nađ, and N. Mišković, "Marus - a marine robotics simulator," *OCEANS 2022, Hampton Roads*, pp. 1–7, 2022. [Online]. Available: https://api.semanticscholar.org/CorpusID:254908555

[11] T. Moore and D. Stouch, "A generalized extended Kalman filter implementation for the robot operating system," in *Intelligent Autonomous Systems 13: Proceedings of the 13th International Conference IAS-13*. Springer, 2016, pp. 335–348.

Co-funded by the European Union

SeaClear2.0 is co-funded by the European Union under the Horizon Europe Programme (Grant Agreement 101093822). Views and opinions expressed herein are those of the author(s) and do not necessarily reflect those of the European Union or European Climate, Infrastructure and Environment Executive Agency (CINEA). Neither the European Union nor the granting authority can be held responsible for them

# A SeaDragon USV parameters

Table 4: Estimated model parameters for the SeaDragon shuttle tender USV

| **SeaDragon USV Parameters** | |
|---|---|
| **Parameter Description** | **Value** |
| Length ($L$) | $5.5\,\mathrm{m}$ |
| Length of Waterline ($L_{wl}$) | $5.5\,\mathrm{m}$ |
| Weight of the Vessel | $450\,\mathrm{kg}$ |
| Beam ($B$) | $2.2\,\mathrm{m}$ |
| Payload mass ($m_p$) | $350\,\mathrm{kg}$ |
| Payload location w.r.t. to COG | [-1.5 0 0] $\mathrm{m}$ |
| Centre of Gravity w/o equipment($rg$) | [2, 0, 0.0] $\mathrm{m}$ |
| Yaw Time Constant ($T_{yaw}$) | $3.236\,\mathrm{s}$ |
| Maximum Forward Speed ($U_{max}$) | $9\,\mathrm{knot}$ |
| Maximum Static Forward Thrust ($T_{max}$) | $31\,\mathrm{kg}$ |
| Maximum Static Backwards Thrust ($T_{min}$) | $-31\,\mathrm{kg}$ |
| Centerline to Waterline Centroid ($y_{pont}$) | $0.9\,\mathrm{m}$ |
| Waterline Area Coefficient $Cw_{pont}$ | $0.7883$ |
| Block Coefficient $Cb_{pont}$ | 0.8998 |
| Draft (front) $d_f$ | $0.10\,\mathrm{m}$ |
| Draft (back) $d_b$ | $0.21\,\mathrm{m}$ |


Co-funded by the European Union

SeaClear2.0 is co-funded by the European Union under the Horizon Europe Programme (Grant Agreement 101093822). Views and opinions expressed herein are those of the author(s) and do not necessarily reflect those of the European Union or European Climate, Infrastructure and Environment Executive Agency (CINEA). Neither the European Union nor the granting authority can be held responsible for them